

Supporting Information

Highly Dispersed Ag nanoparticles in Ti-MOFs with partial ligand removal for catalytic conversion of CO₂

Contents

- 1. Experimental Section**
- 2. Characterizations of Catalysts**
- 3. Catalysis Details**
- 4. References**

1. Experimental Section.

1.1 Materials and methods

Materials and Methods. All substrates were used as received from commercial suppliers unless otherwise stated. Chemicals were purchased from Sigma-Aldrich, Chempur, TCI, or Alfa Aesar.

X-ray diffraction (XRD) using a Bruker D8 Advance X-ray diffractometer (Cu K α radiation, $\lambda = 1.5418\text{\AA}$) in the range of $5-50^\circ(2\theta)$. Scanning electron microscope (SEM) experiments used JSM-7610F Plus record. Transmission electron microscopy (TEM) were performed on JEM-F200. The spectra of the Advanced Fourier Transform Infrared Spectrometer were measured with a ThermoFisher 6700 instrument (KBr pellets). N₂ sorption isotherm at 77 K were carried out on Micromeritics 3Flex Surface Characterization Analyzer. Thermogravimetric analyses (TGA) were performed at a ramp rate of 10 °C/min in a nitrogen flow with an SDTQ600 instrument. X-ray photoelectron spectroscopy (XPS) signals were collected on a Thermo ESCALAB Xi⁺ spectrometer. ¹H NMR data were collected on a Bruker Avance III 400 MHz spectrometer at ambient temperature. ¹³C NMR data were collected on a Bruker Avance III 500 MHz spectrometer at ambient temperature.

1.2 Syntheses and methods

Synthesis procedure of NH₂-MIL-125(0.5)^[1]

The mixed ligand mof, i.e., NH₂-MIL-125 (0.5), was prepared by addition of both BDC and BDC- NH₂ ligands in the same proportions, and in a single synthesis, TTIP (0.592 mL), BDC- NH₂ (271.7 mg) were dispersed by sonication for 20 mins into a solution of 18 mL of DMF and 2 mL of methanol (V_{DMF}/ V_{MeOH}=9:1) solution, after which BDC (249 mg) was added to the above solution. The mixture was then transferred to a 15 mL Teflon-lined stainless steel autoclave and reacted at 150 °C for

24 h. The product was collected by centrifugation and washed three times with DMF and methanol. Finally, NH₂-MIL-125 (0.5) was activated by removing the solvent under vacuum at 70 °C for 12 h.

Synthesis procedure of d-NH₂-MIL-125(0.5)

Heat treatment mof. Sample NH₂-MIL-125(0.5) was heated to 300 °C at a constant rate of increase in temperature (10 °C • min⁻¹) and held at this temperature for 5 h. In this case, the sample was cooled to room temperature.

Synthesis procedure of Ag/NH₂-MIL-125(0.5)^[2]

A series of Ag/d-NH₂-MIL-125 materials with varying silver concentrations were synthesized through the following procedure: First, 40 mg of d-NH₂-MIL-125(0.5) was dispersed in 2 mL of methanol, followed by the addition of 10 mL of a 0.3 mM AgNO₃-methanol solution. The mixture was stirred at 60 °C for 12 h under a N₂ atmosphere in the dark to facilitate silver deposition. Subsequently, photodeposition was performed by irradiating the mixture under a 300 W Xe lamp for 30 min to obtain Ag MOF-1. Using the same method, two additional samples—Ag MOF-2 (0.15 mM AgNO₃-methanol solution) and Ag MOF-3 (0.45 mM AgNO₃-methanol solution)—were prepared to achieve different silver loadings. After synthesis, the precipitate was collected by centrifugation and repeatedly washed with methanol to remove unreacted species. The product was then activated under vacuum at 100 °C for 10 h to eliminate residual solvents, followed by storage under a N₂ atmosphere. Finally, inductively coupled plasma (ICP) analysis was employed to quantify the silver content in each sample, confirming the successful incorporation of silver.

2.Characterizations of Catalysts.

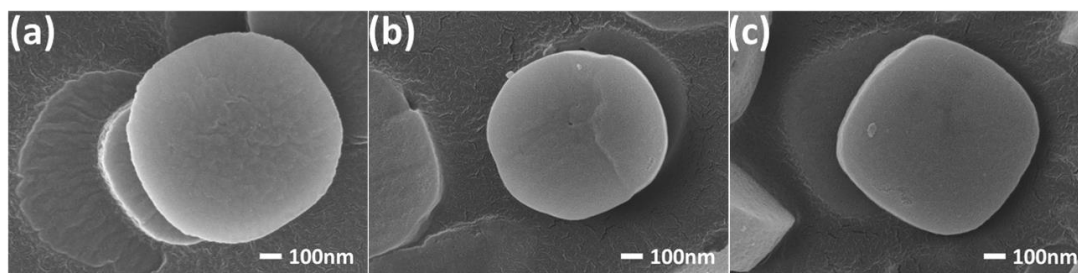


Fig.S1. SEM image of (a) NH₂-MIL-125(0.5), (b) d-NH₂-MIL-125(0.5), (c) Ag MOF-2.

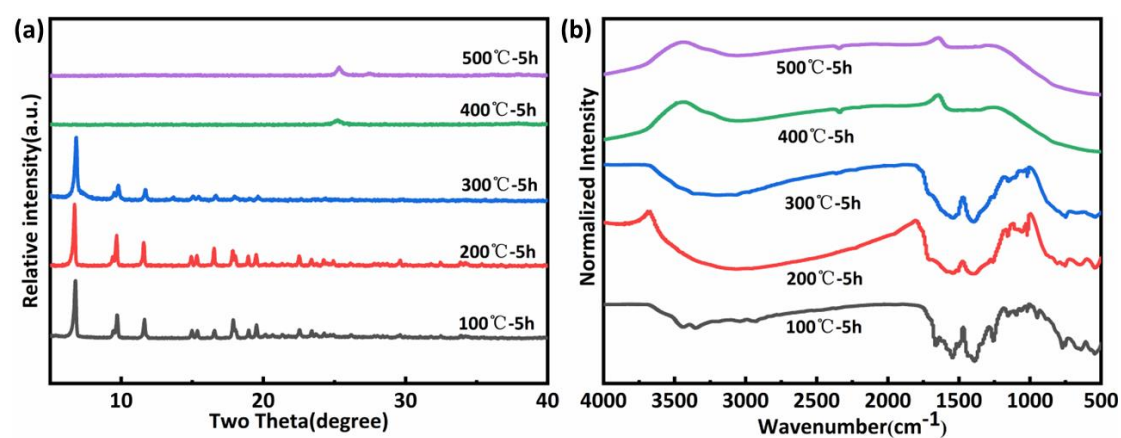


Fig.S2. (a) XRD and (b) IR pattern of NH₂-MIL125(0.5) from 100 °C to 500 °C.

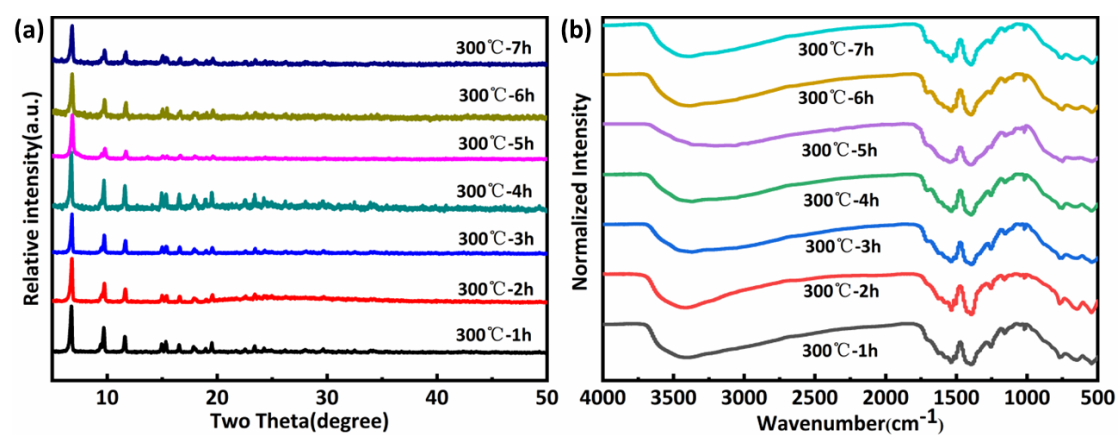


Fig.S3. (a) XRD and (b) IR patterns for heat-treated NH₂-MIL-125(0.5) at 300 °C for 1-7 h.

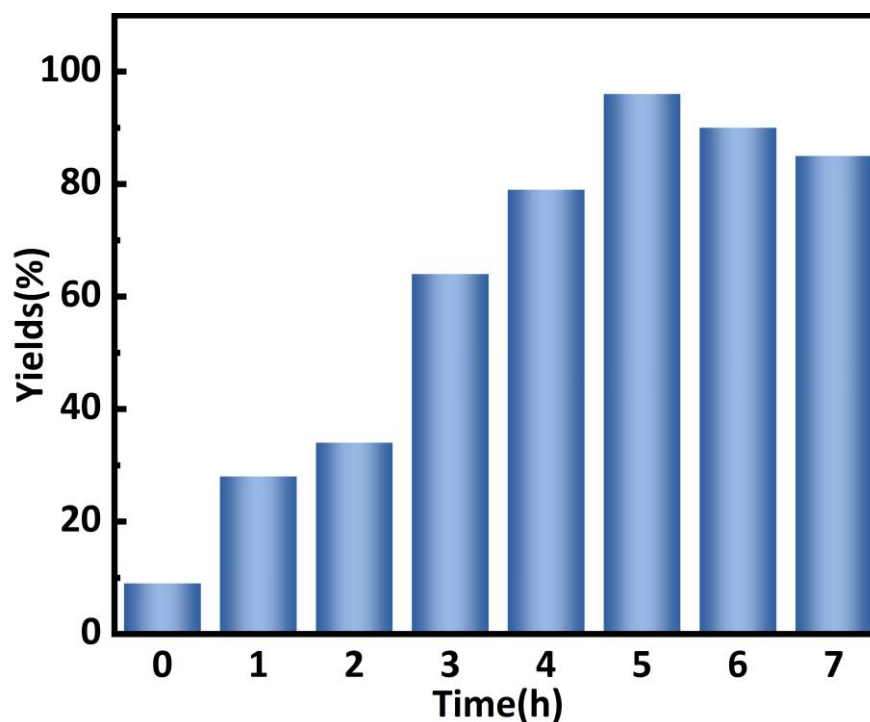


Fig.S4. NH₂-MIL-125(0.5) was treated at 300 °C for 1-7 h and loaded with equal amounts of AgNO₃ (0.13, 1.26, 2.7, 3.23, 4.81, 4.3, 4.14 wt% of Ag in all the samples tested by ICP), which determined the best reaction time for optimal calcination at the optimal calcination temperature of 300 °C. The optimum reaction time at the optimum calcination temperature of 300 °C was determined. The significantly higher yields obtained by heating the samples up to 5 h seem to be related to the difference in the amount of porosity due to the different calcination times of the samples. As the treatment time was prolonged new active sites were continuously introduced, which promoted the deposition of Ag NPs as well as the adsorption of the substrate, thus facilitating the reaction. When the time was prolonged to a certain time, the reaction rate decreased instead, probably due to the collapse of some pores and blockage of some active sites.

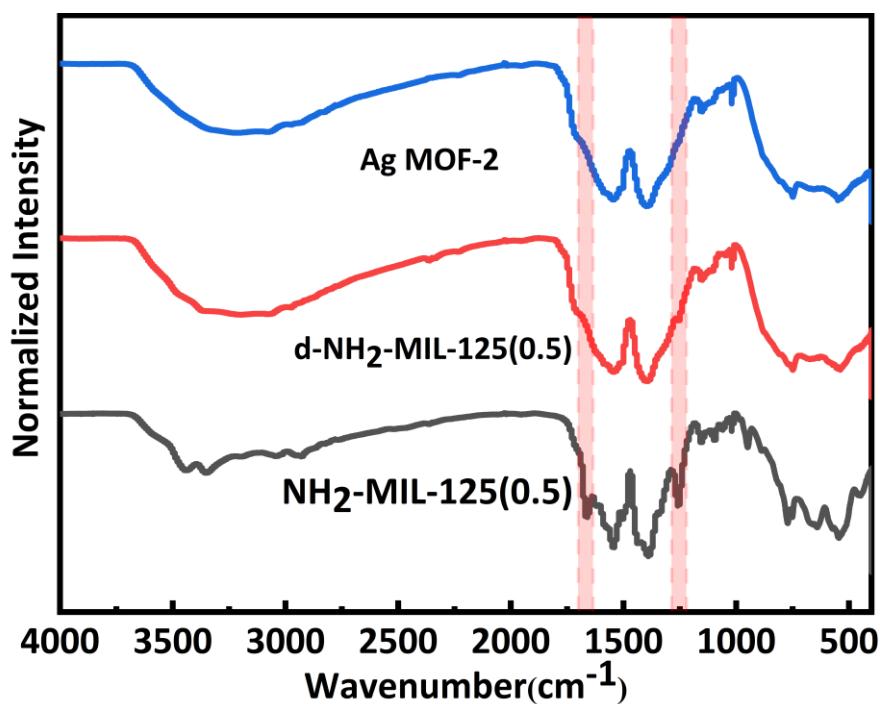


Fig.S5. FT-IR spectra of NH₂-MIL-125(0.5), d-NH₂-MIL-125(0.5) and Ag MOF-2.

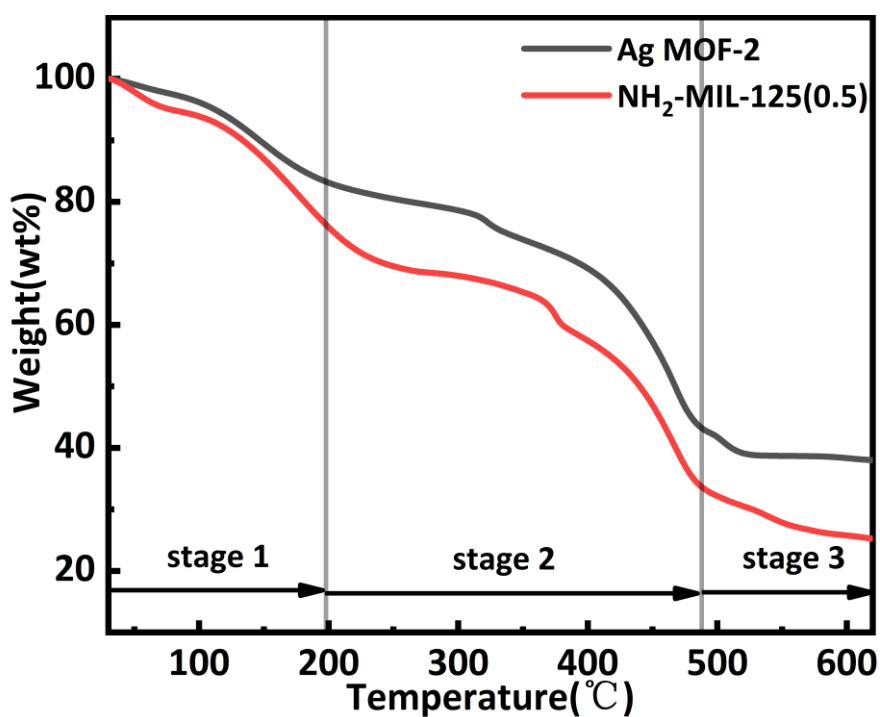


Fig.S6. TGA pattern of NH₂-MIL-125(0.5) and Ag MOF-2, using a ramp rate of 10 $^{\circ}\text{C} \cdot \text{min}^{-1}$ in air. Stage I indicates the removal of solvents (DMF); Stage II marks the selective removal of BDC-NH₂; stage III shows the degradation of BDC.

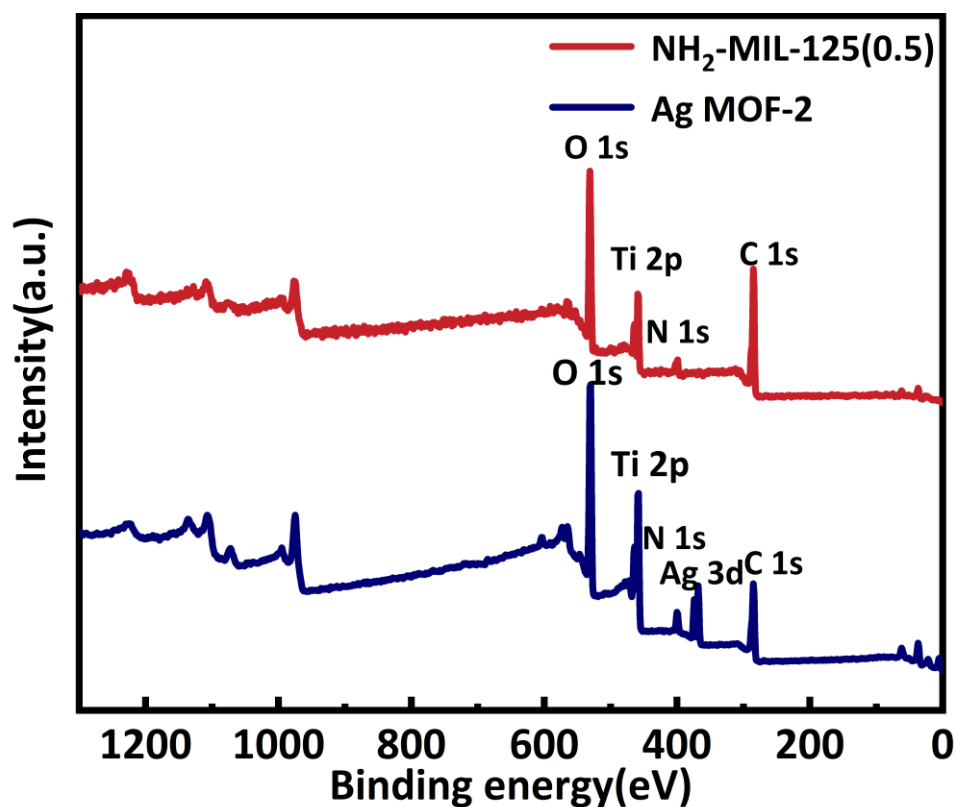


Fig.S7. XPS survey spectra of $\text{NH}_2\text{-MIL-125(0.5)}$ and Ag MOF-2 .

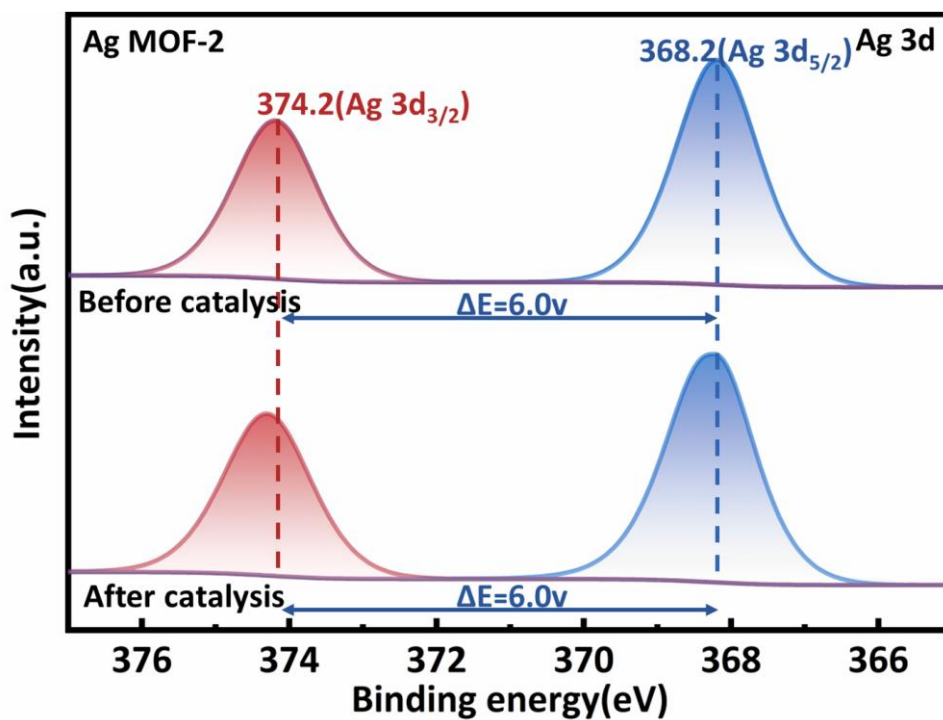


Fig.S8. High-resolution XPS spectrum of Ag 3d for Ag MOF-2 .

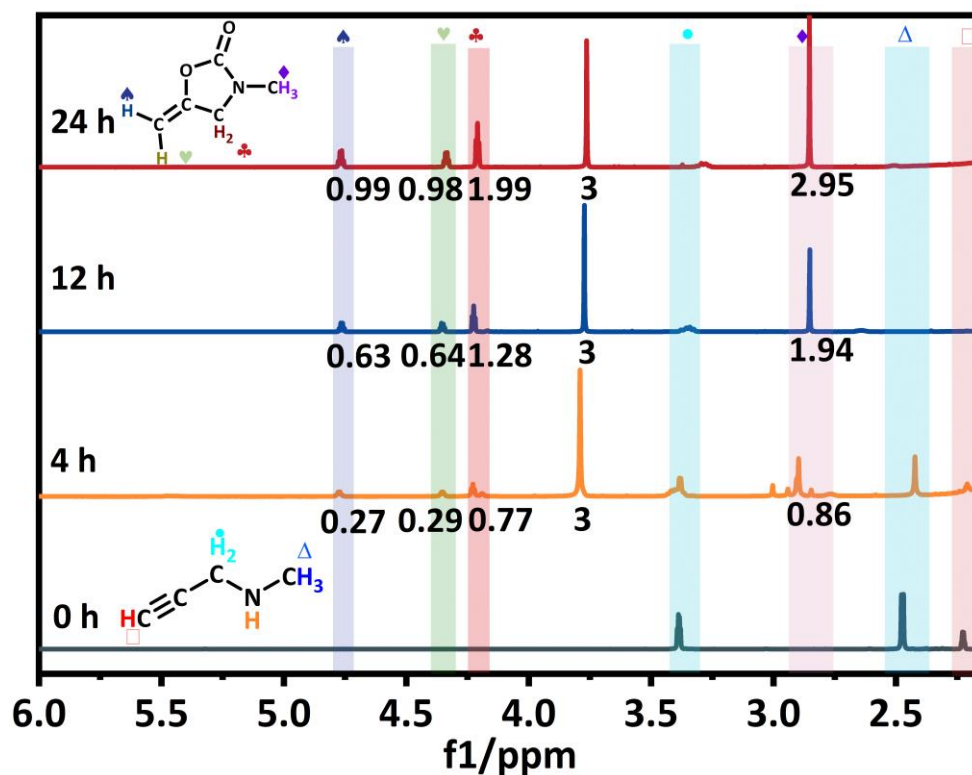


Fig.S9. ^1H NMR monitoring of the cyclization reaction of the substrate with CO_2 catalyzed by propargylic amine.

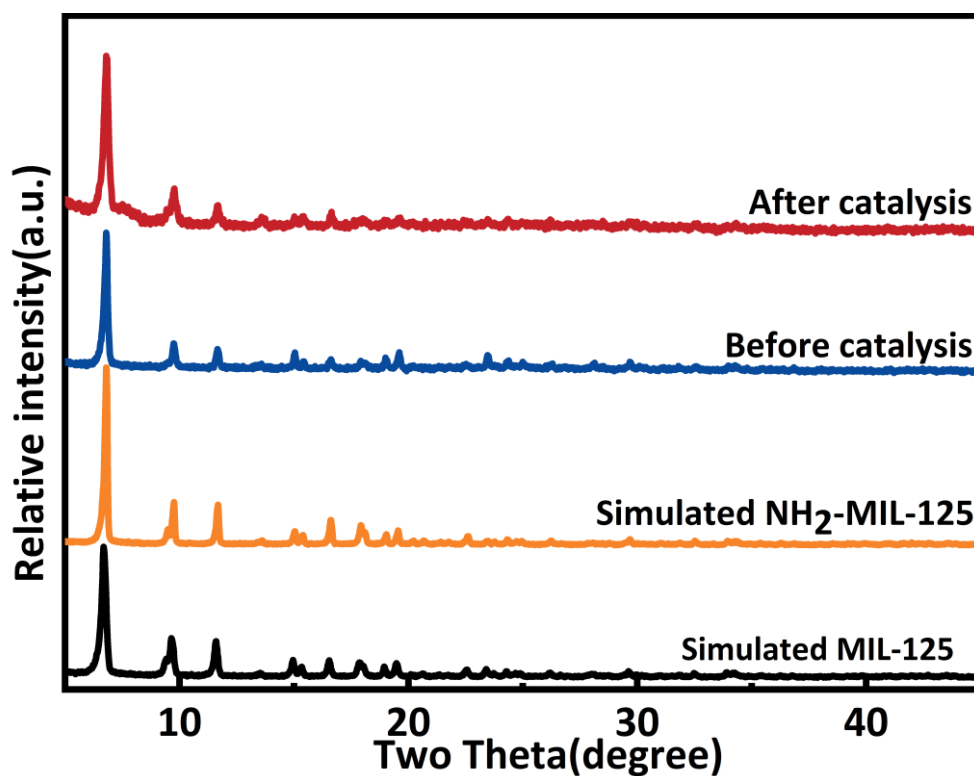


Fig.S10. The PXRD spectra of Ag MOF-2 before catalysis and after catalysis.

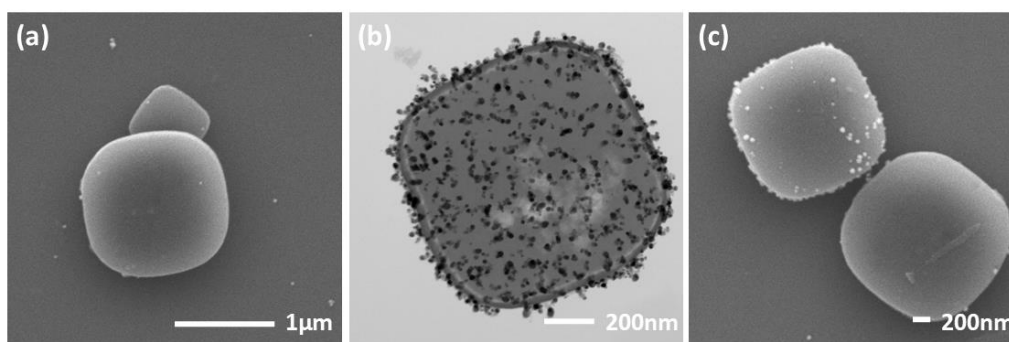


Fig.S11. Characterization of Ag MOF-2 after catalytic cycles: (a) SEM and (b) TEM images of Ag MOF-2 after the carboxylative cyclization of N-methylpropargylamine with CO₂; (c) SEM image of Ag MOF-2 following the carboxylation cycle of phenylacetylene.

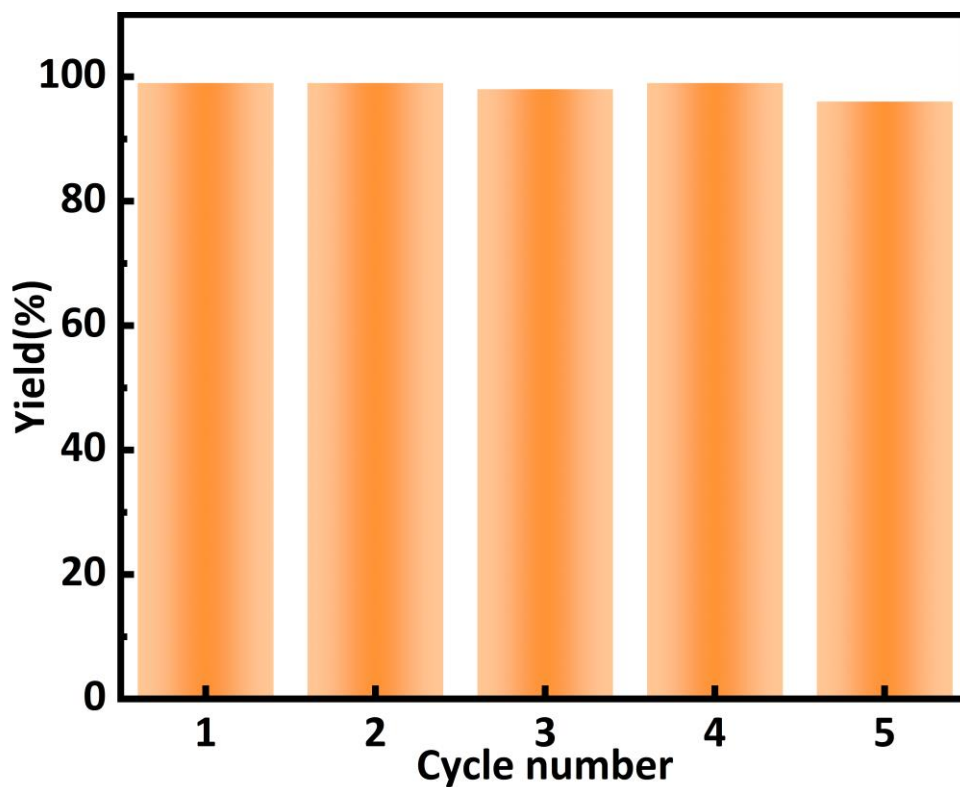


Fig.S12. Recycling tests of the catalyst Ag MOF-2 for the reaction of terminal alkynes with CO₂.

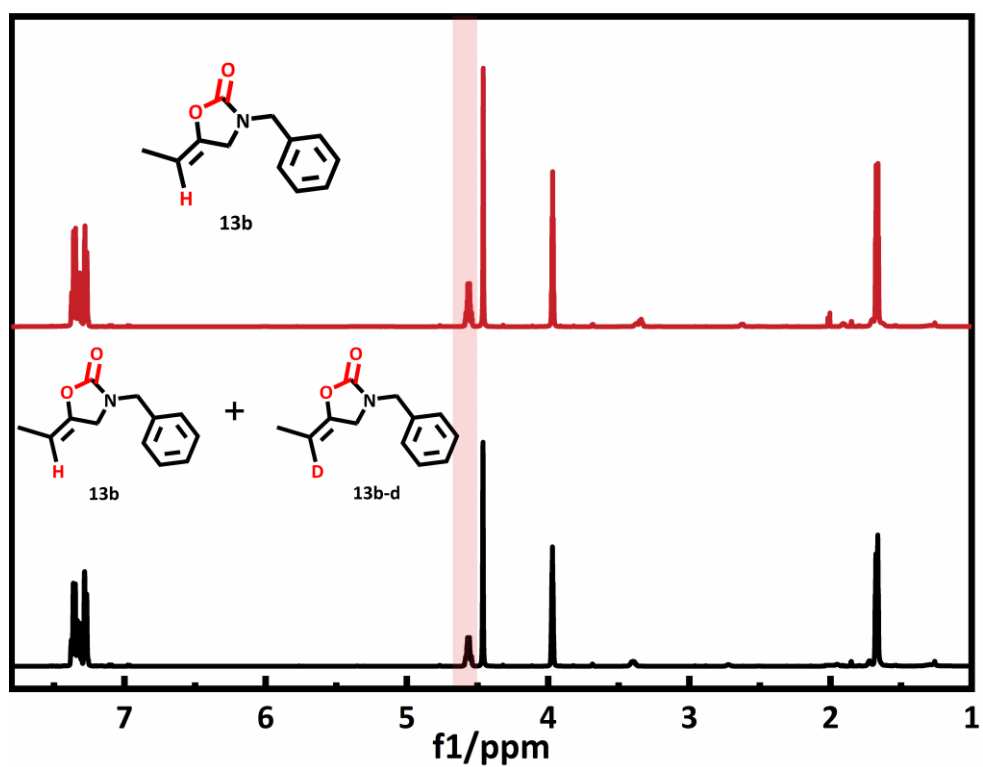


Fig.S13. The comparison between the ^1H NMR spectra of 13b/13b-d and 13b.

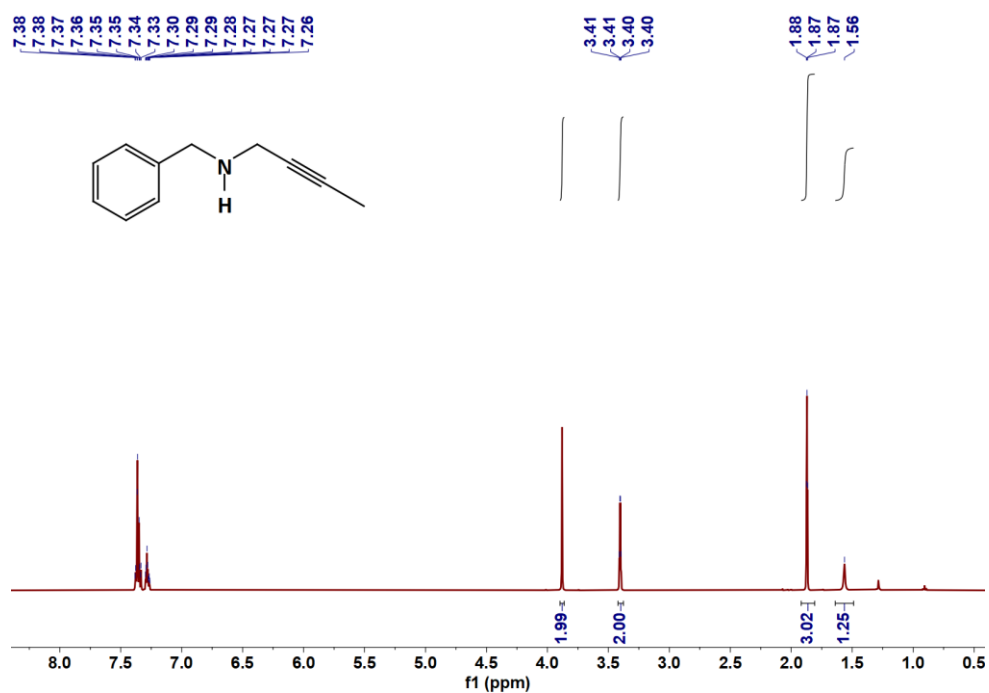


Fig.S14. The ^1H NMR spectrum of 13a.

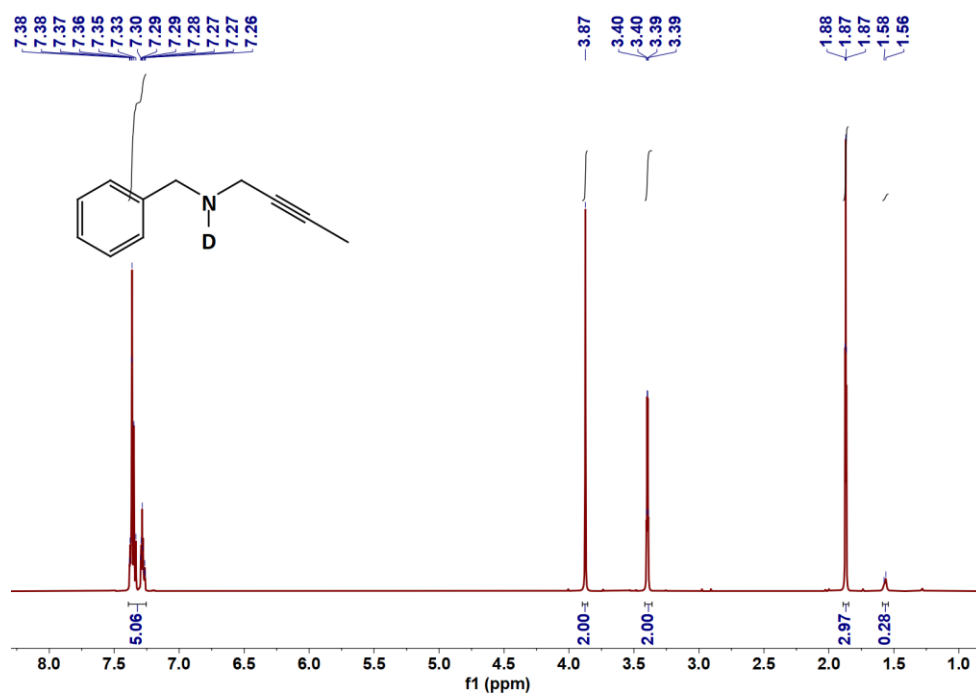


Fig.S15. The ¹H NMR spectrum of 13a-d.

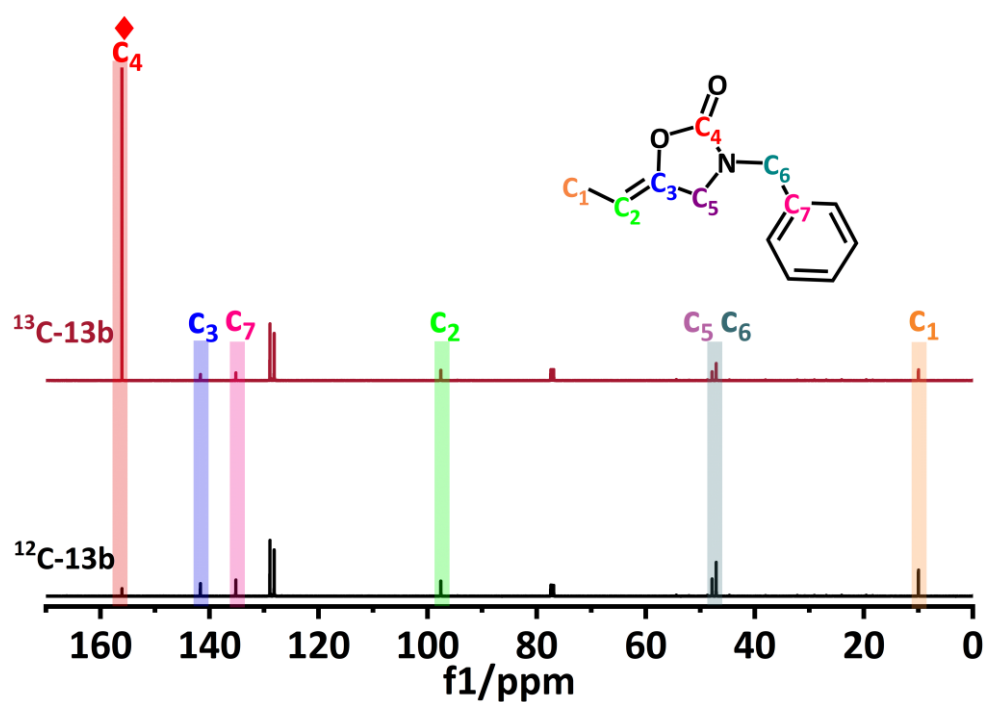


Fig.S16. Comparative ¹³C NMR Analysis of ¹³C-Isotope-Labeled Cyclic Carboxylation Product 13b

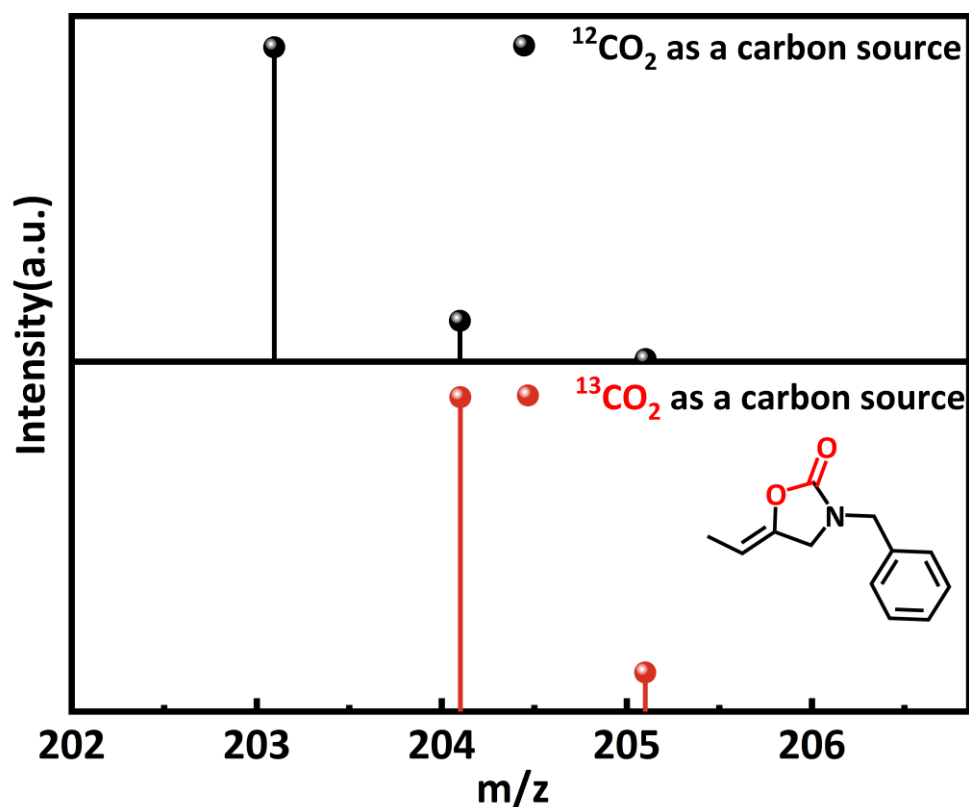


Fig.S17. Mass spectra of the 13b ($m/z = 203.1$) formed when using $^{13}\text{CO}_2$ (red), $^{12}\text{CO}_2$ (black).

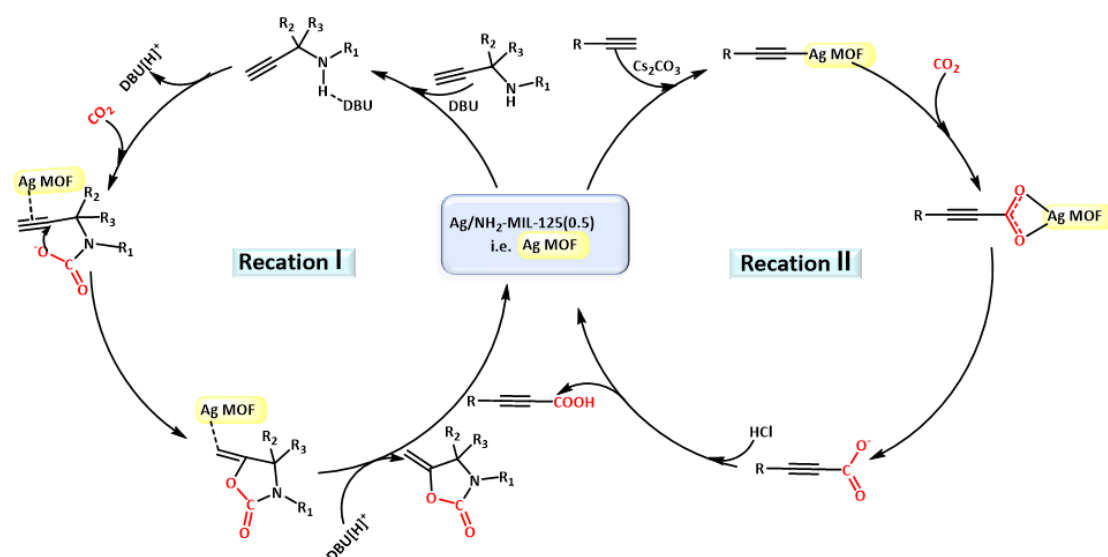


Fig.S18. Proposed mechanism of carboxylative cyclization of propargylamines with CO_2 and the reaction between terminal alkynes with CO_2 catalyzed by $\text{Ag}/\text{NH}_2\text{-MIL-125(0.5)}$ (Ag MOF).^[3]

Table S1. Comparison of catalytic activities for for carboxylative cyclization of propargylamines with CO₂ between Ag MOF-2 and reported catalytic systems.

Entry	Catalyst	T(°C)	Time(h)	Solvent	Base	Yield(%)	Ref.
1	Ag MOF-2	50	24	CH ₃ CN	DBU	99	This work
2	Ag@NPOP-1	40	2	CH ₃ CN	DBU	86	[4]
3	Ag@TpPa-1	60	18	CH ₃ CN	DBU	96	[5]
4	AgN@COF	55	10	H ₂ O:EtOH	DMAB	95	[6]
5	Cu NPs@COF	50	12	CH ₃ CN	DBU	95	[7]
6	Cu-TSP	50	24	CH ₃ CN	DBU	99	[8]
7	Cu ₂ O@ZIF-8	40	12	CH ₃ CN	DBU	99	[9]
8	Cu ₂ O@MIL-101(Cr)-DABCO	R.T.	12	CH ₃ CN	DBU	96.1	[10]
9	Ag-MOF-1	25	24	CH ₃ CN	DBU	95	[11]
10	TOS-Ag4	25	96	CH ₃ CN	DBU	93	[12]
11	TNS-Ag8	25	180	CH ₃ CN	DBU	76	[12]
12	Ag ₂₇ -MOF	25	240	CH ₃ CN	DBU	97	[13]
13	Ag/Azo-Por-TAPM	40	10	CH ₃ CN	DBU	97	[14]

Table S2. Comparison of catalytic activities for alkyne carboxylation reactions between Ag MOF-2 and reported catalytic systems.

Catalyst	T(°C)	Time(h)	Solvent	Base	Pressure	Yield(%)	Ref.
Ag MOF-2	50°C	12h	DMF	Cs ₂ CO ₃	1atm	99	This work
Ag@NPOP-2	60°C	12h	DMSO	Cs ₂ CO ₃	1 atm	92.1	[15]
HM-CeO ₂ -Ag	R.T.	40h	DMF	Cs ₂ CO ₃	1 atm	98.5	[16]
Ag@MIL-100(Fe)	50°C	15h	DMF	Cs ₂ CO ₃	1 atm	94.6	[17]
Ag@ZIF-8	40°C	20h	DMF	Cs ₂ CO ₃	1 atm	97	[18]
Ag@MIL-101	50°C	15h	DMF	Cs ₂ CO ₃	1 atm	96.5	[19]
[Gd ₃ Cu ₁₂ I ₁₂ (IN) ₉ (DMF) ₄] _n	80°C	4h	EC	Cs ₂ CO ₃ ;n-Bul	1 atm	80	[20]
Ag@Pybpy-COF	50°C	12h	DMF	Cs ₂ CO ₃	1 atm	98	[21]
Pd _{0.2} -Cu _{0.8} /MIL-101	25°C	24h	DMSO	Cs ₂ CO ₃	60atm	96	[22]
ZIF-8@Au ₂₅ @ZIF-67	50°C	12h	DMF	Cs ₂ CO ₃	1 atm	99	[23]
Ag@UIO-66	50°C	15h	DMF	Cs ₂ CO ₃	1 atm	97.7	[17]
JNM-Au-1	50°C	2h	DMF	Cs ₂ CO ₃	1 atm	91	[24]

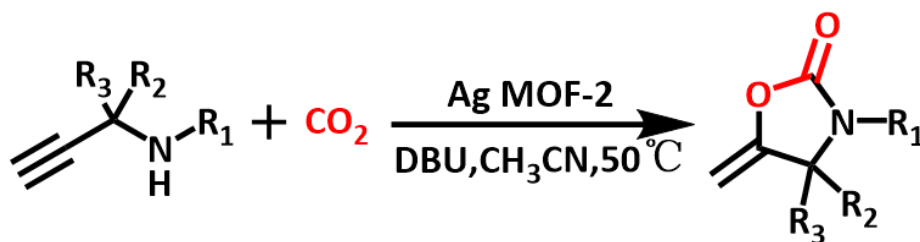
Table S3. ICP-OES analysis of Ag MOF-1, Ag MOF-2, Ag MOF-3.

Sample	Analyte	Concentration	Intensity	Content
Ag MOF-1	Ag 328.068	16.15mg/L	133138.4	3.23wt%
Ag MOF-2	Ag 328.08	28.93mg/L	3080736.2	4.81wt%
Ag MOF-3	Ag 328.08	32.97mg/L	2717298.5	6.1wt%

Table S4. Summary of the S_A and pore volume of NH_2 -MIL-125(0.5), d- NH_2 -MIL-125(0.5) and Ag MOF-2.

Samples	Apparent specific surface area(m^2g^{-1})	NLDFT Micropore volume(cm^3g^{-1})	NLDFT Total pore volume(cm^3g^{-1})
NH_2 -MIL-125(0.5)	1259.2	0.01822	0.4596
d- NH_2 -MIL-125(0.5)	825.4	0.00366	0.3165
Ag MOF-2	544.61	0.0234	0.2150

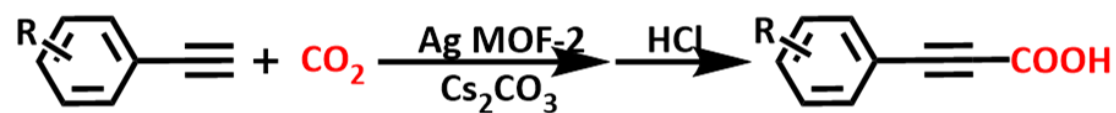
Table S5. Control experiments for the catalytic carboxylation of propargylic amines with CO₂.



Entry	deviation from standard conditions	Yield (%) ^b
1	Standard condition ^a	99
2	MeOH instead of CH ₃ CN	31
3	CHCl ₃ instead of CH ₃ CN	40
4	DMSO instead of CH ₃ CN	69
5	no catalyst	0
6	no DBU	3
7	Air instead of CO ₂	5
8	N ₂ instead of CO ₂	0
9	TEA instead of DBU	68
10	Room temperature	40
11	CF ₃ COOAg	41
12	AgNO ₃	59
13	AgBF ₄	54
14	AgOAc	63
15	NH ₂ -MIL-125(0.5)	2
16	d-NH ₂ -MIL-125(0.5)	0
17	Ag MOF-1	65
18	Ag MOF-3	73

Standard conditions^a: 1a (0.3 mmol), Ag MOF-2 (catalyst, 5 mg), 0.03 mmol (10 mol%) of DBU, CH₃CN (3 mL), 50 °C, 24 h, CO₂ (balloon). The yields were determined using ¹H NMR spectroscopy^[4].

Table S6. Controlled Experiments for the Ag MOF-2 catalyzed carboxylation of alkynes.



Entry	deviation from standard conditions	Yield (%) ^b
1	Standard condition ^b	99
2	no catalyst	0
3	no Cs ₂ CO ₃	0
4	K ₂ CO ₃ instead of Cs ₂ CO ₃	46
5	N ₂ instead of CO ₂	0
6	Room temperature	30
7	NH ₂ -MIL-125(0.5)	Trace
8	CH ₃ CN instead of DMF	69
9	DMSO instead of DMF	80

Standard conditions^b: 1c (1 mmol, 1 equiv), Ag MOF-2 (catalyst 5 mg), Cs₂CO₃ (1.5 equiv), DMF (3 mL), CO₂ (1.0 atm), 50 °C, 12 h. The yields were determined using ¹H NMR spectroscopy^[5].

3. Catalysis Details

3.1 Catalytic Synthesis of Substrates

N-methylpropargylamine (1a): The substrate 1a was purchased from Energy Chemical and used without further purification.

N-(prop-2-yn-1-yl) butan-1-amine (2a) and N-(cyclohexylmethyl) prop-2-yn-1-amine (3a): The substrate 2a was prepared according to previous reference.^[7,25]

Synthesis and Characterization of Propargylic Amines (4a-12a): One drop of acetic acid was added to the mixture of propargylamine (12 mmol, 0.661 g) and benzaldehyde (13 mmol, 1.38 g) in 20mL methanol. The solution was stirred at room temperature for 24 hours. Then, the mixture was cooled to 0 °C, and NaBH₄ (18mmol, 0.68g) was added in portions. The mixture was allowed warmed to room temperature and stirred for 1h. The solution was evaporated to dryness and 100mL water was added. The aqueous phase was extracted with CH₂Cl₂ (50 mL×2) and then the organic phase was extracted with 1 M HCl (50 mL×3). NaHCO₃ was added to neutralize the solution and the mixture was extracted with CH₂Cl₂ (50 mL×2). The organic extracts were washed with brine (50 mL) and dried (MgSO₄). The filtrate was concentrated under reduced pressure, and further purification via silica gel chromatography to afford the pure products.

Synthesis and Characterization of N-2-Butyn-1-ylbenzenemethanamine (13a): To synthesize the target compound, first add 1-bromobut-2-yne (1.5 mmol) dropwise to benzylamine (9.02 mmol) at 0 °C. After the addition is complete, allow the reaction mixture to warm to room temperature and stir for 17 h. Upon completion of the reaction, quench the mixture by adding aqueous 1 M NaOH (4 mL/mmol) and diethyl ether (Et₂O, 4 mL/mmol), then separate the organic and aqueous layers. To ensure

complete extraction, wash the aqueous layer twice with additional Et₂O (2 × 4 mL/mmol). Combine all organic layers and wash them with brine to remove residual impurities. Dry the organic phase over anhydrous MgSO₄, filter, and concentrate the solution under reduced pressure to obtain the crude product. Finally, purify the crude material by flash column chromatography using a silica gel stationary phase and a hexane/ethyl acetate (80:20) eluent system to isolate the desired compound.^[26]

Synthesis and Characterization of Benzenemethanamine-d, N-2-butyn-1-yl-(13a-d): First, dissolve N-benzyl but-2-yn-1-amine (301 mg, 1.89 mmol) in CH₃OD (3.5 mL) and stir the mixture at room temperature for 2 h to allow deuterium exchange. After concentrating the solution in vacuo, repeat the deuteration process by redissolving the residue in fresh CH₃OD (3.0 mL) and stirring for another 1 hour at room temperature. Finally, remove the solvent in vacuo to obtain the deuterated product, N-benzyl but-2-yn-1-amine-d₁, with high isotopic purity.^[27]

3.2 Catalytic Reaction Procedure

Catalytic cyclic carboxylation of propargylic amines with CO₂: A mixture of MOF catalyst (5 mg), propargylamine (0.3 mmol), and DBU (0.1 equiv.) in CH₃CN (3 mL) was added to a Schlenk tube. The reaction system was purged with CO₂ gas for 10 min and then stirred at 50 °C under a CO₂ atmosphere (0.1 MPa) for 24 h. After completion, the catalyst was separated by filtration, and the resulting filtrate was concentrated under reduced pressure. The crude product was diluted with CDCl₃ (0.5 mL) for ¹H NMR analysis to determine the catalytic conversion rate. The recovered catalyst was washed thoroughly with methanol, activated under vacuum at 100 °C for 10 h, and subsequently reused for further catalytic cycles.

Procedure for catalytic carboxylation of terminal alkynes: A mixture of Ag MOF-2 (5 mg), Cs₂CO₃ (1.5 mmol), and terminal alkyne (1 mmol) was dispersed in

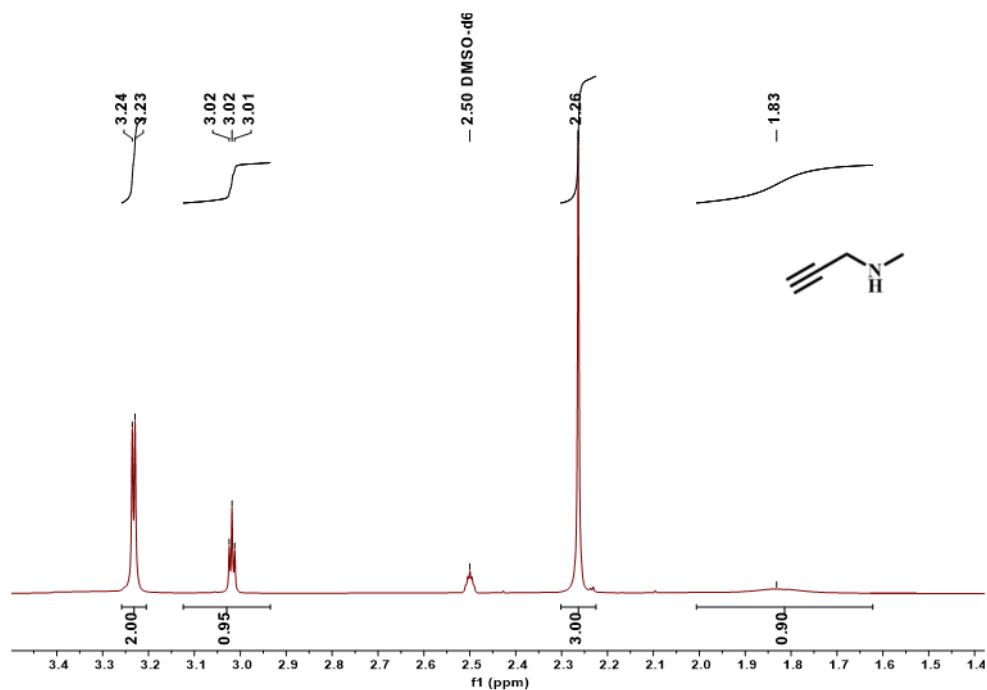
DMF (3 mL) in a Schlenk tube. The reaction system was purged with CO₂ for 10 min and then heated at 50 °C under 0.1 MPa CO₂ atmosphere with stirring for 12 h. Upon reaction completion, the mixture was diluted with H₂O (10 mL) and extracted with dichloromethane (3 × 15 mL). The aqueous layer was acidified to Ph=1 using 1M HCl, followed by extraction with ethyl acetate (3 × 5 mL). The combined organic layers were dried over anhydrous Na₂SO₄, filtered, and concentrated under reduced pressure to afford the target product.

Cyclic experiment details: To ensure a fair comparison between the heterogeneous MOF catalyst and homogeneous AgNO₃ system, parallel experiments were conducted under identical reaction conditions (0.3 mmol propargylamine, 0.1 equiv DBU, 3 mL CH₃CN, 50 °C, 0.1 MPa CO₂, 24 h). Distinct recycling protocols were implemented according to each catalyst's physical properties: For the MOF catalyst, the solid was recovered by filtration, thoroughly washed with methanol to remove adsorbed species, and reactivated under vacuum at 100 °C for 10 h to restore catalytic sites before reuse. For the catalytic cycle experiments of the carboxylative cyclization between terminal alkynes and CO₂, all experimental procedures remain identical except for the reaction conditions. For the soluble AgNO₃ catalyst, the entire reaction mixture was concentrated via rotary evaporation, followed by washing with fresh CH₃CN to eliminate organic residues. The recovered AgNO₃ was then dried under reduced pressure at 45 °C for 4 h in the dark with continuous N₂ protection to prevent reduction to metallic silver.

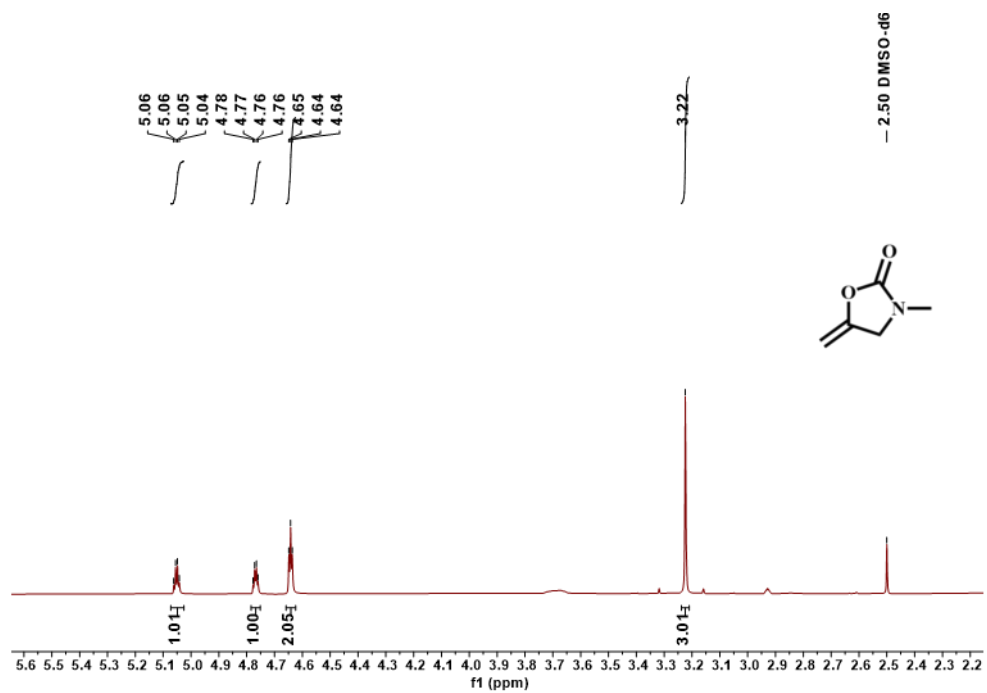
Isotope labeling experiments: In a Schlenk tube, a mixture of MOF catalyst (5 mg), N-2-butyn-1-ylbenzenemethanamine (0.3 mmol), and DBU (0.1 equiv) in CH₃CN (3 mL) was degassed via three freeze-pump-thaw cycles and charged with ¹³CO₂ (1 atm). The reaction was stirred at 50 °C for 24 h. Upon completion, the mixture was diluted

with EtOAc (30 mL), filtered, and concentrated in vacuo. The crude product was purified by column chromatography (petroleum ether/EtOAc, 10:1) to afford the carboxylative cycloaddition product as a pale yellow oil.

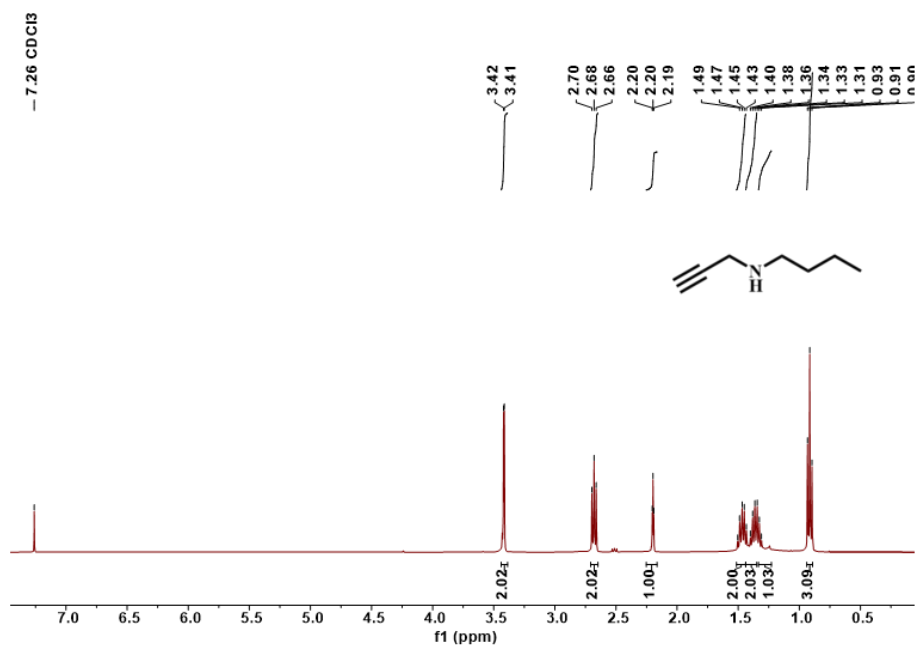
N-Methylmaleimide (1a): ^1H NMR (400 MHz, $\text{DMSO-}d_6$) δ 3.24 (d, $J = 2.4$ Hz, 2H), 3.02 (t, $J = 2.4$ Hz, 1H), 2.26 (s, 3H), 1.83 (s, 1H).



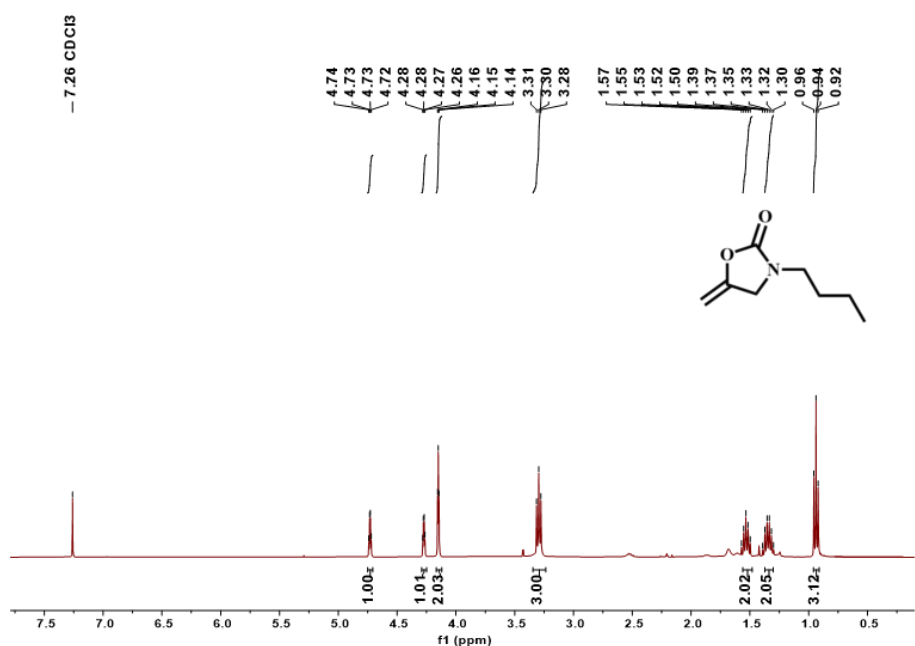
3-methyl-5-methyleneoxazolidin-2-one (1b): ^1H NMR (400 MHz, $\text{DMSO-}d_6$) δ 5.05 (q, $J = 2.7$ Hz, 1H), 4.77 (q, $J = 2.4$ Hz, 1H), 4.64 (t, $J = 2.4$ Hz, 2H), 3.22 (s, 3H).



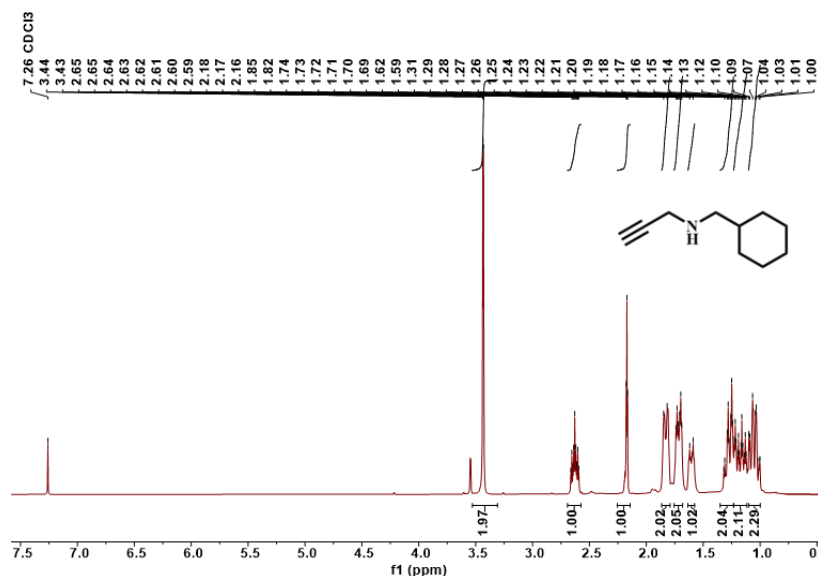
N-(prop-2-yn-1-yl) butan-1-amine (2a): ^1H NMR (400 MHz, Chloroform-*d*) δ 3.42 (d, $J = 2.5$ Hz, 2H), 2.68 (t, $J = 7.1$ Hz, 2H), 2.20 (t, $J = 2.4$ Hz, 1H), 1.48 (dd, $J = 15.0, 6.4$ Hz, 2H), 1.44 – 1.35 (m, 2H), 1.32 (d, $J = 7.1$ Hz, 1H), 0.91 (t, $J = 7.3$ Hz, 3H).



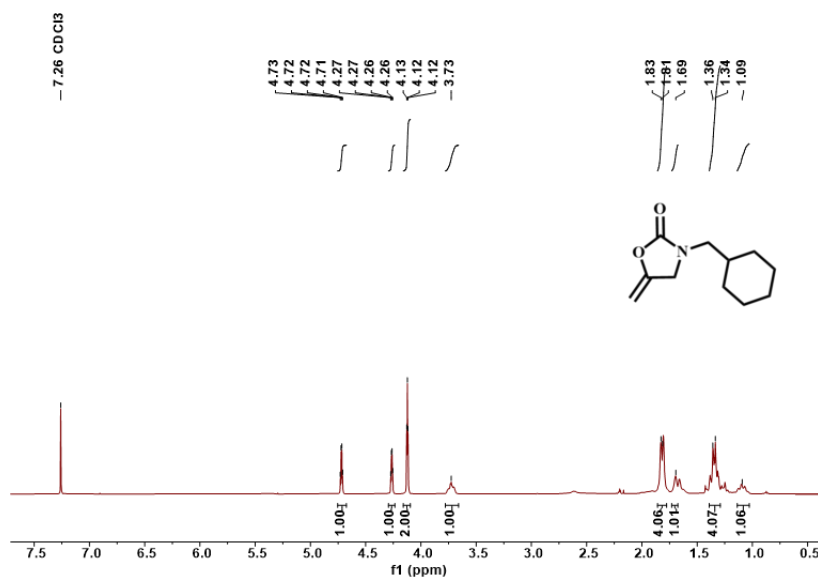
3-butyl-5-methyleneoxazolidin-2-one (2b): ^1H NMR (400 MHz, Chloroform-*d*) δ 4.75 (q, $J = 2.7$ Hz, 1H), 4.30 (q, $J = 2.2$ Hz, 1H), 4.17 (t, $J = 2.4$ Hz, 2H), 3.32 (t, $J = 7.3$ Hz, 3H), 1.55 (q, $J = 7.6$ Hz, 2H), 1.40 – 1.33 (m, 2H), 0.96 (t, $J = 7.3$ Hz, 3H).



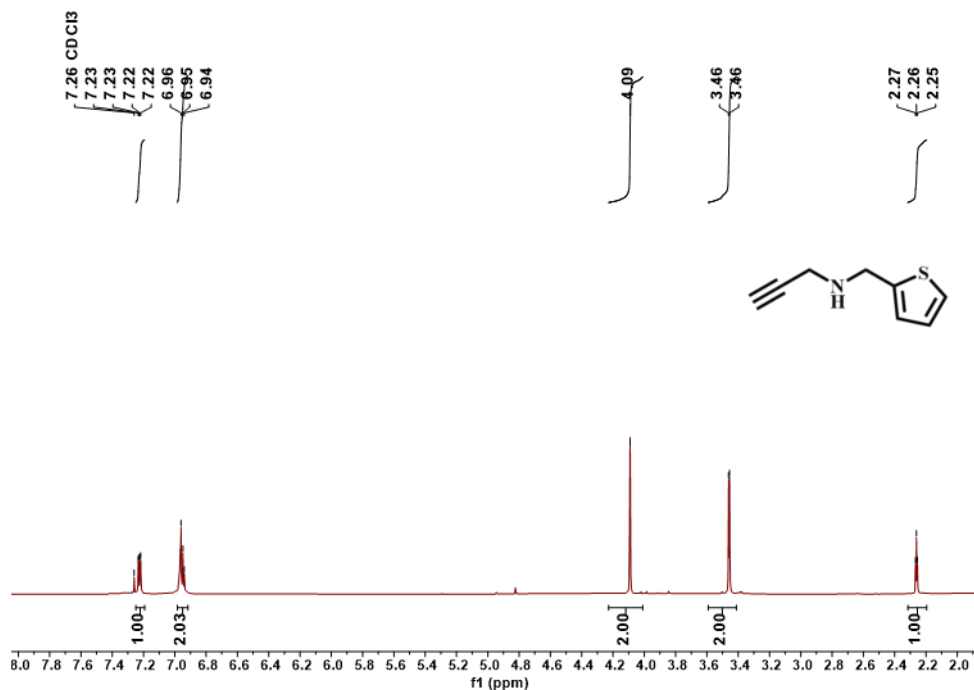
N-(cyclohexylmethyl)prop-2-yn-1-amine (3a): ^1H NMR (400 MHz, Chloroform-*d*) δ 3.43 (d, $J = 2.5$ Hz, 2H), 2.63 (tt, $J = 10.3, 3.7$ Hz, 1H), 2.17 (t, $J = 2.4$ Hz, 1H), 1.83 (d, $J = 12.2$ Hz, 2H), 1.71 (dt, $J = 12.6, 3.6$ Hz, 2H), 1.60 (d, $J = 12.4$ Hz, 1H), 1.28 (ddd, $J = 15.8, 9.3, 3.3$ Hz, 2H), 1.17 (ddt, $J = 24.4, 12.1, 3.4$ Hz, 2H), 1.10 – 1.00 (m, 2H).



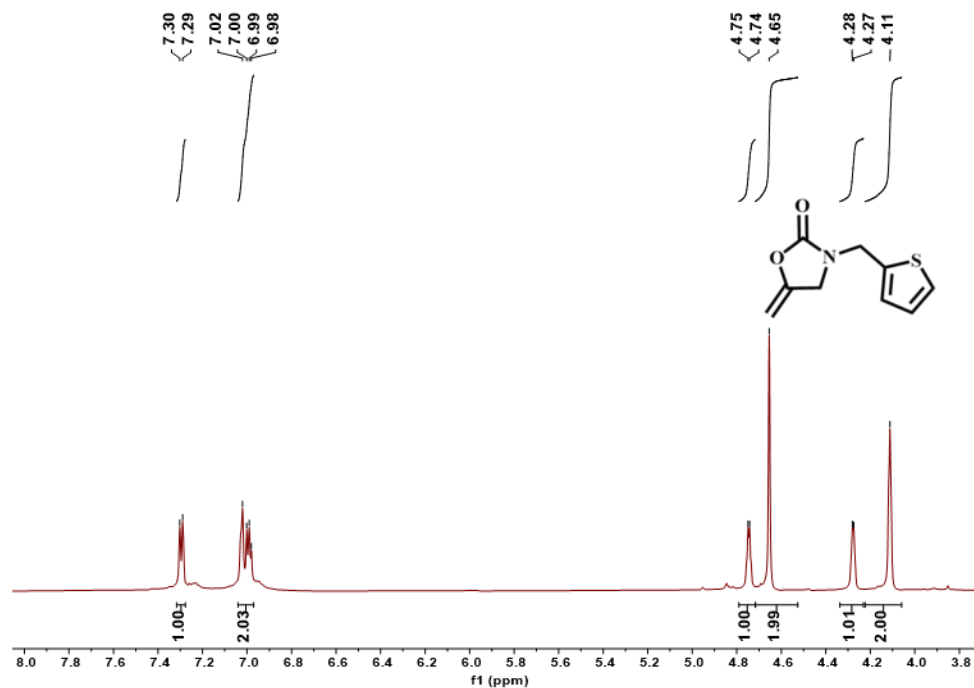
3-(cyclohexylmethyl)-5-methyleneoxazolidin-2-one (3b): ^1H NMR (400 MHz, Chloroform-*d*) δ 4.73 (q, $J = 2.7$ Hz, 1H), 4.28 (q, $J = 2.3$ Hz, 1H), 4.14 (t, $J = 2.4$ Hz, 2H), 3.74 (s, 1H), 1.83 (d, $J = 8.5$ Hz, 4H), 1.71 (s, 1H), 1.36 (d, $J = 8.8$ Hz, 4H), 1.12 (s, 1H).



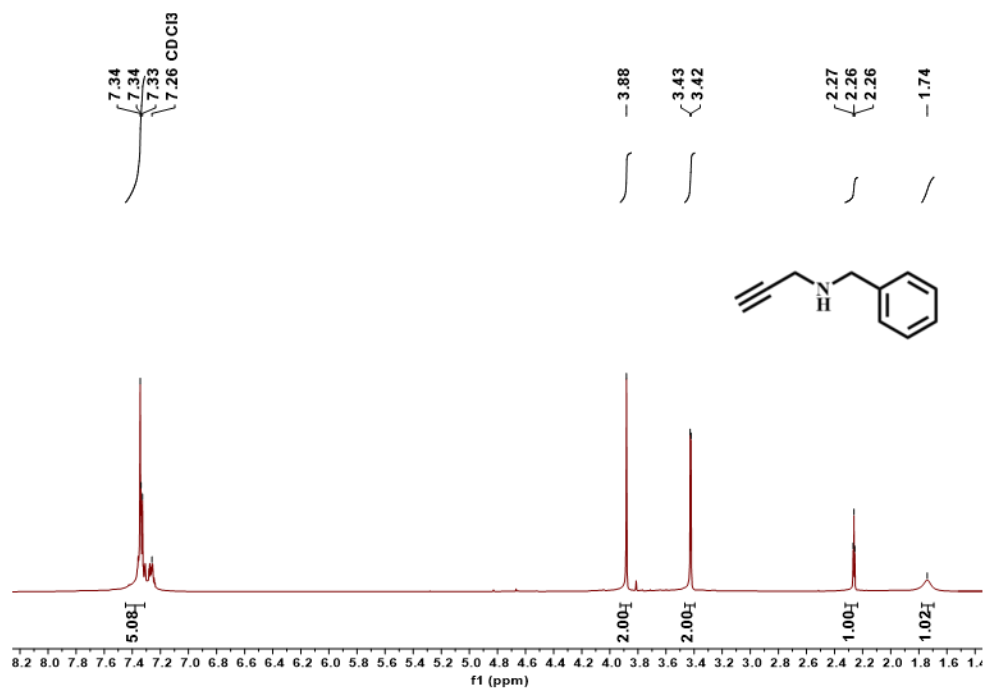
N-(thiophen-2-ylmethyl) prop-2-yn-1-amine (4a): ^1H NMR (400 MHz, Chloroform-*d*) δ 7.23 (dd, $J = 4.9, 1.5$ Hz, 1H), 6.98 – 6.92 (m, 2H), 4.09 (s, 2H), 3.46 (d, $J = 2.5$ Hz, 2H), 2.26 (t, $J = 2.4$ Hz, 1H).



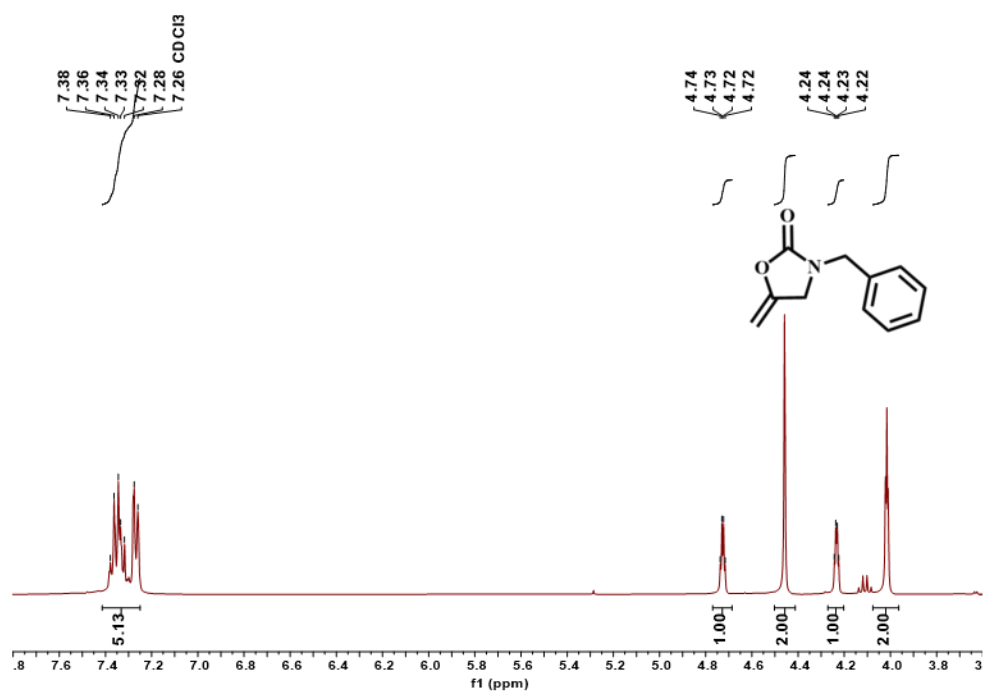
5-methylene-3-(thiophen-2-ylmethyl) oxazolidin-2-one (4b): ^1H NMR (400 MHz, Chloroform-*d*) δ 7.30 (d, $J = 5.3$ Hz, 1H), 7.00 (dd, $J = 10.2, 5.7$ Hz, 2H), 4.75 (d, $J = 2.9$ Hz, 1H), 4.65 (s, 2H), 4.28 (d, $J = 2.7$ Hz, 1H), 4.11 (s, 2H).



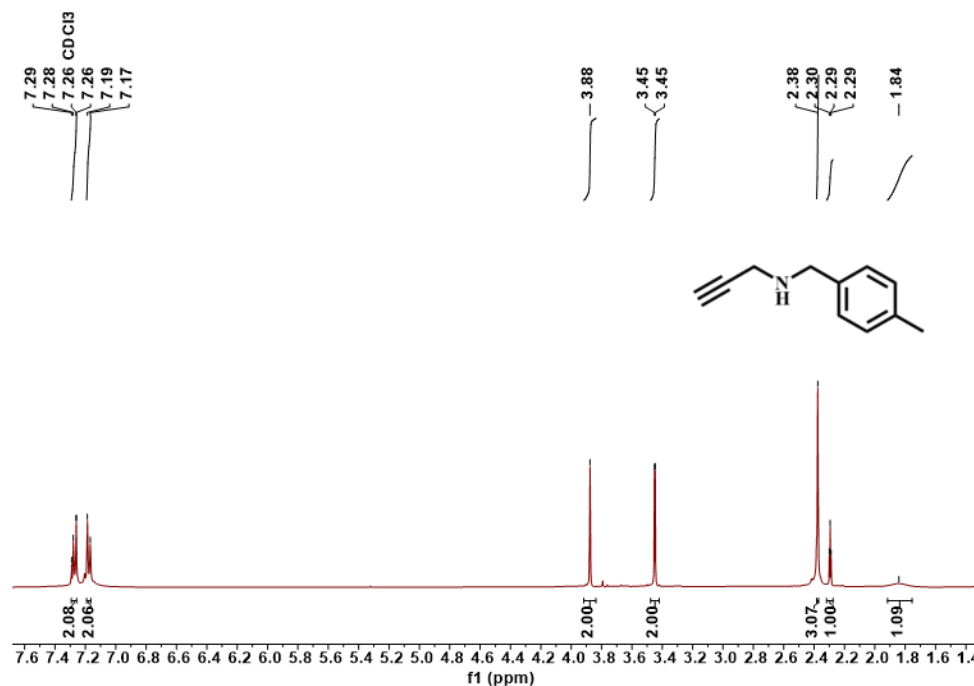
N-benzylprop-2-yn-1-amine (5a): ^1H NMR (400 MHz, Chloroform-*d*) δ 7.45 – 7.31 (m, 5H), 3.88 (s, 2H), 3.42 (d, $J = 2.4$ Hz, 2H), 2.26 (t, $J = 2.4$ Hz, 1H), 1.74 (s, 1H).



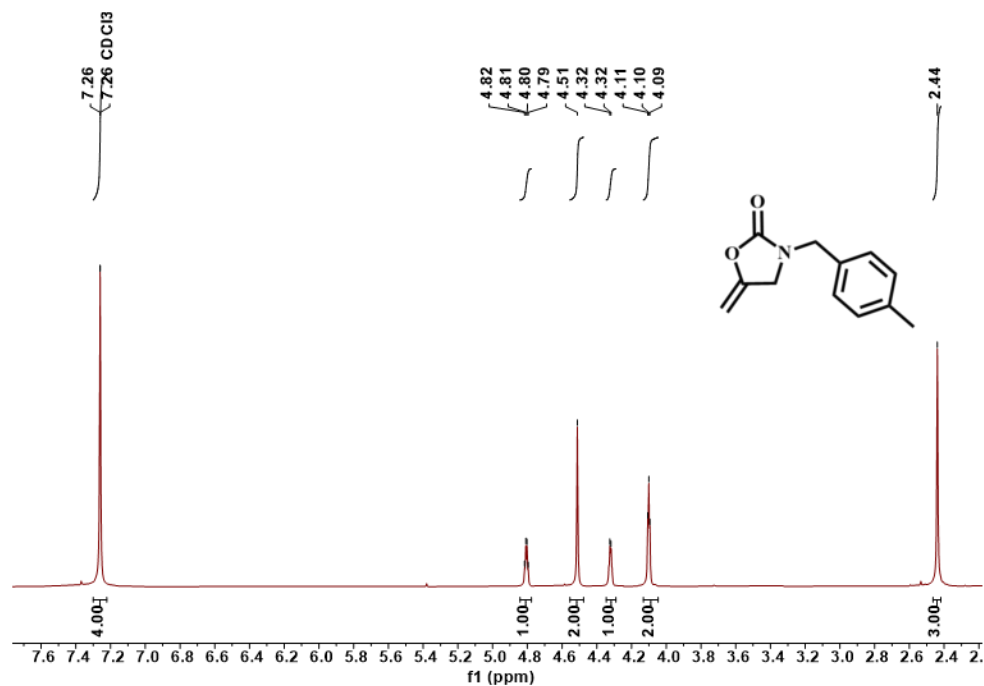
3-benzyl-5-methyleneoxazolidin-2-one (5b): ^1H NMR (400 MHz, Chloroform-*d*) δ 7.41 – 7.25 (m, 5H), 4.73 (q, $J = 2.8$ Hz, 1H), 4.46 (s, 2H), 4.23 (q, $J = 2.5$ Hz, 1H), 4.02 (t, $J = 2.4$ Hz, 2H).



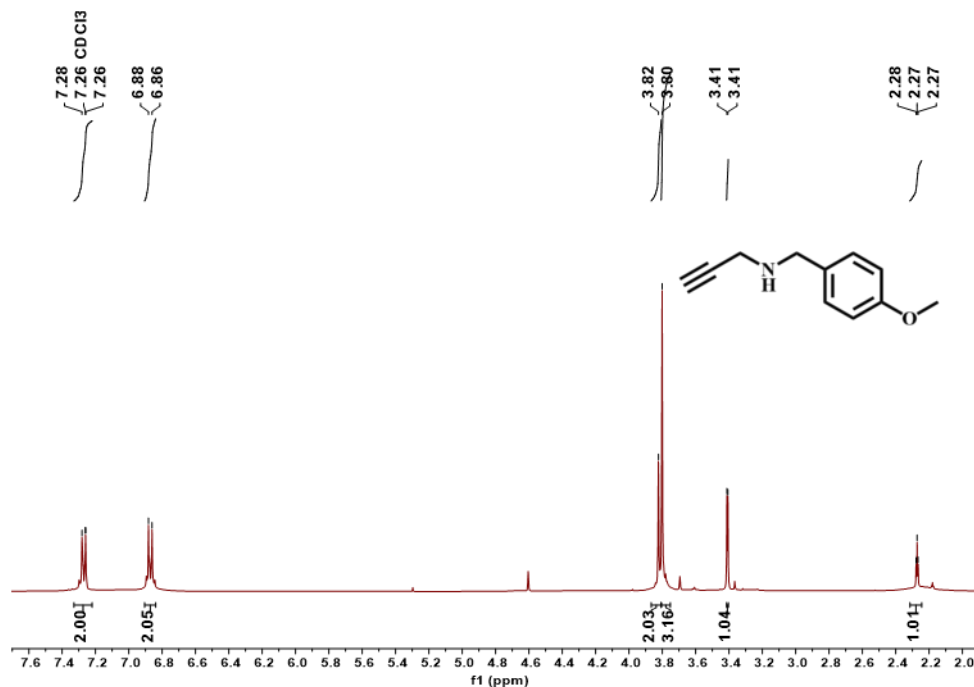
N-(4-methylbenzyl) prop-2-yn-1-amine (6a): ^1H NMR (400 MHz, Chloroform-*d*) δ 7.28 (d, $J = 8.0$ Hz, 2H), 7.19 (d, $J = 7.7$ Hz, 2H), 3.88 (s, 2H), 3.46 (d, $J = 2.4$ Hz, 2H), 2.38 (s, 3H), 2.30 (t, $J = 2.4$ Hz, 1H), 1.85 (s, 1H).



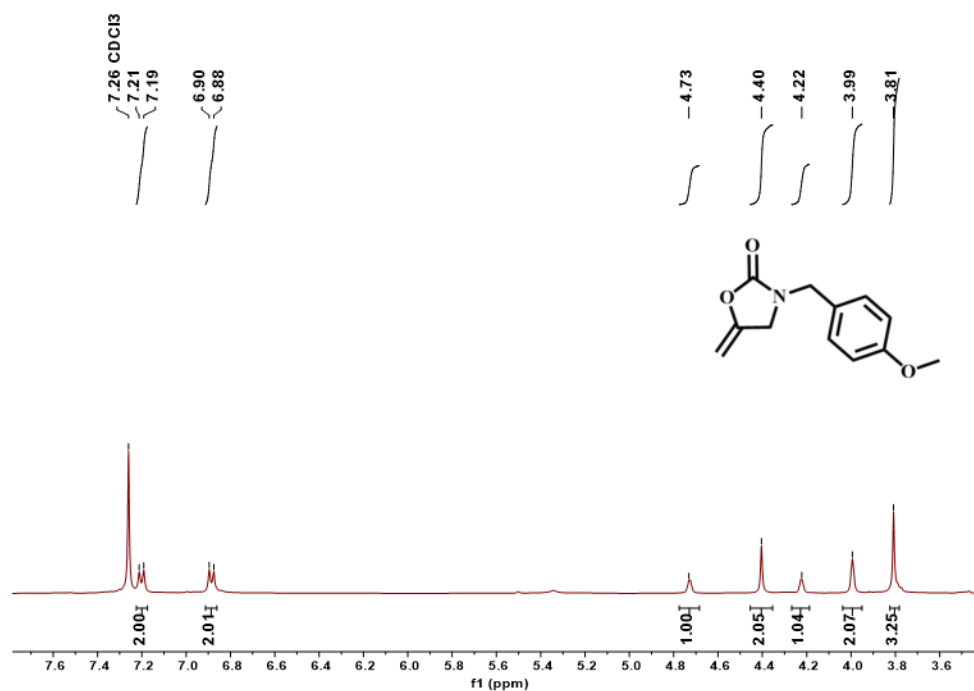
3-(4-methylbenzyl)-5-methyleneoxazolidin-2-one (6b): ^1H NMR (400 MHz, Chloroform-*d*) δ 7.26 (s, 4H), 4.81 (q, $J = 2.8$ Hz, 1H), 4.51 (s, 2H), 4.32 (d, $J = 2.6$ Hz, 1H), 4.10 (t, $J = 2.4$ Hz, 2H), 2.44 (s, 3H).



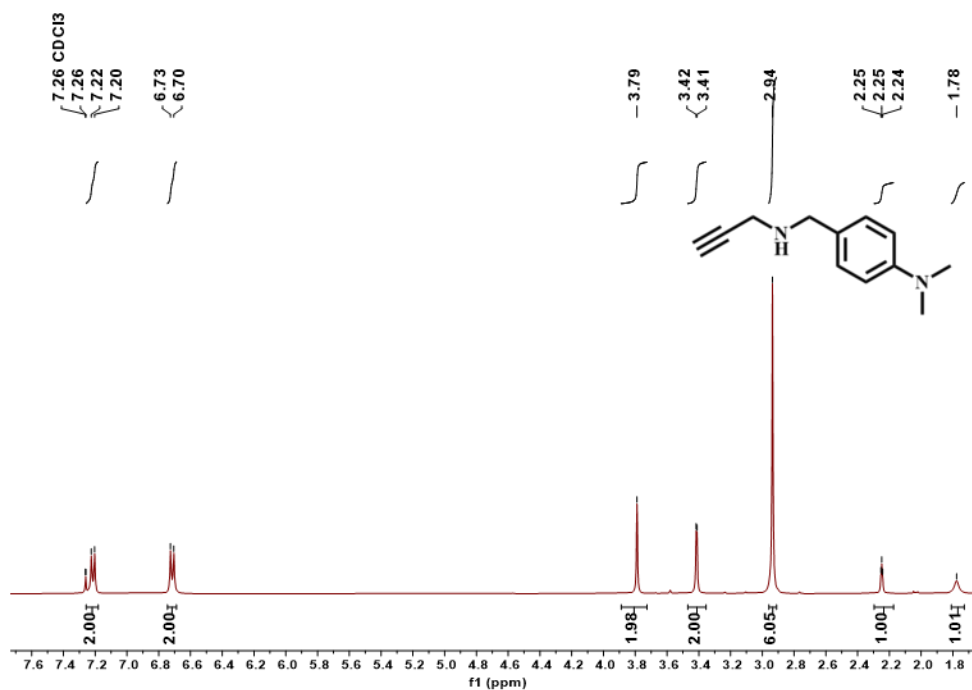
N-(4-methoxybenzyl) prop-2-yn-1-amine (7a): ^1H NMR (400 MHz, Chloroform-*d*) δ 7.27 (d, J = 8.7 Hz, 2H), 6.87 (d, J = 8.7 Hz, 2H), 3.82 (s, 2H), 3.80 (s, 3H), 3.41 (d, J = 2.4 Hz, 1H), 2.27 (t, J = 2.4 Hz, 1H).



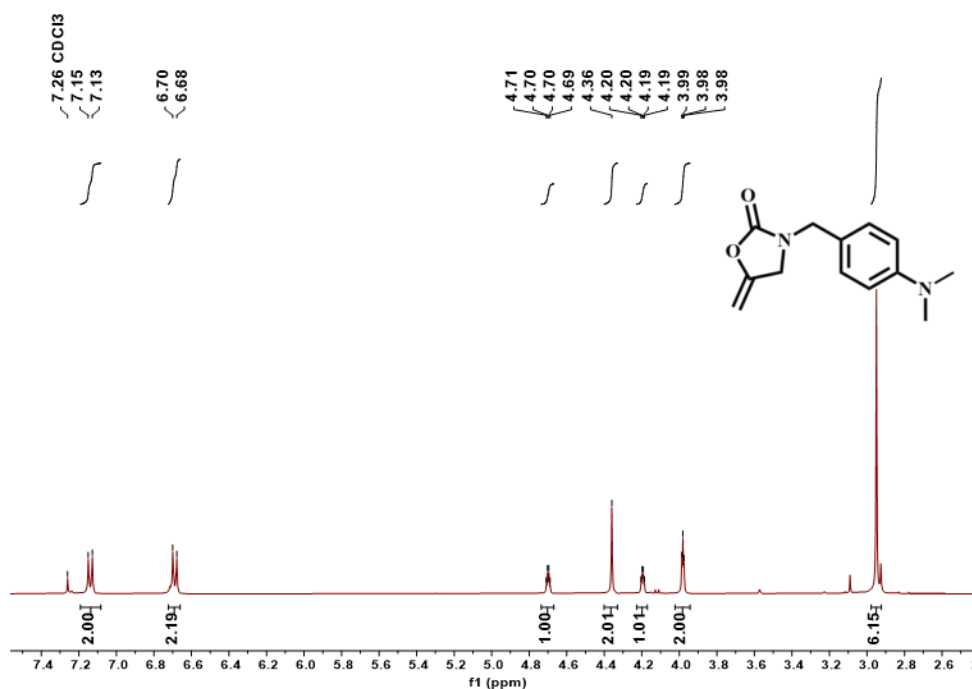
3-(4-methoxybenzyl)-5-methyleneoxazolidin-2-one (7b): ^1H NMR (400 MHz, Chloroform-*d*) δ 7.45 – 7.09 (m, 1H), 6.89 (d, J = 8.4 Hz, 1H), 4.73 (s, 1H), 4.40 (s, 1H), 4.22 (s, 1H), 3.99 (s, 1H), 3.81 (s, 1H).



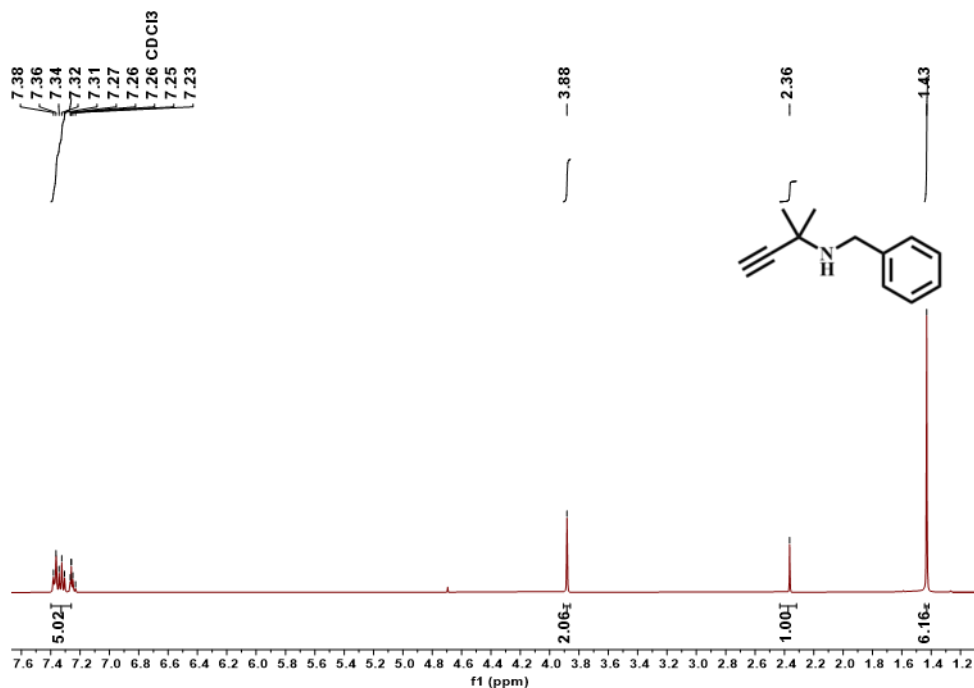
N, N-dimethyl-4-((prop-2-yn-1-ylamino) methyl) aniline (8a): ^1H NMR (400 MHz, Chloroform-*d*) δ 7.24 (d, J = 8.5 Hz, 2H), 6.74 (d, J = 8.5 Hz, 2H), 3.81 (s, 2H), 3.43 (d, J = 2.5 Hz, 2H), 2.96 (s, 6H), 2.27 (t, J = 2.4 Hz, 1H), 1.80 (s, 1H).



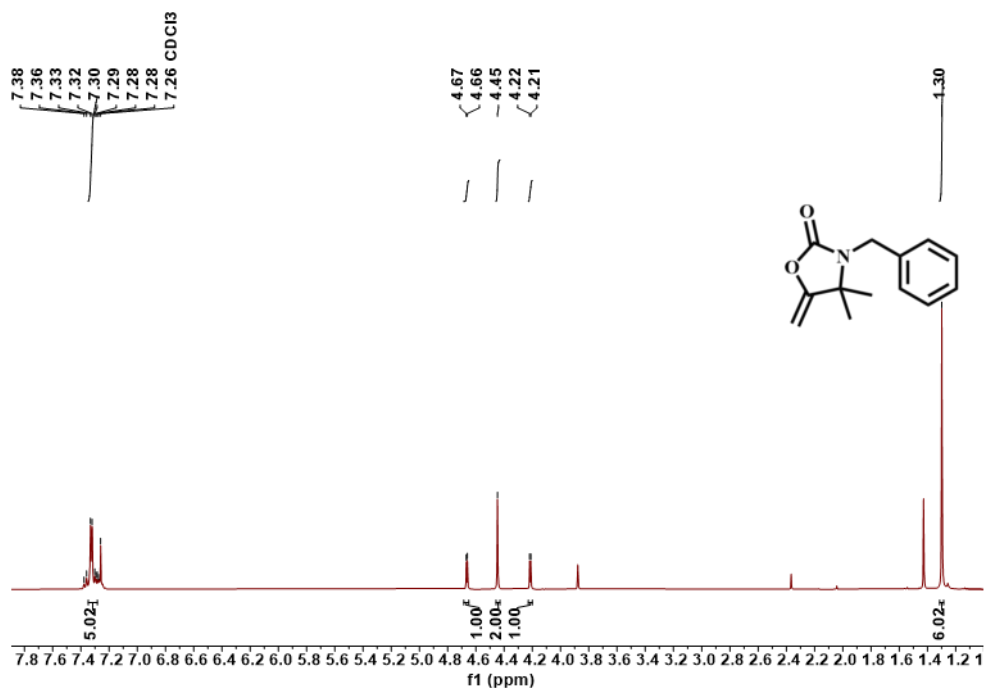
3-(4-(dimethylamino) benzyl)-5-methyleneoxazolidin-2-one (8b): ^1H NMR (400 MHz, Chloroform-*d*) δ 7.20 (d, J = 8.3 Hz, 2H), 6.89 (d, J = 8.4 Hz, 2H), 4.73 (s, 1H), 4.40 (s, 2H), 4.22 (s, 1H), 3.99 (s, 2H), 3.81 (s, 3H).



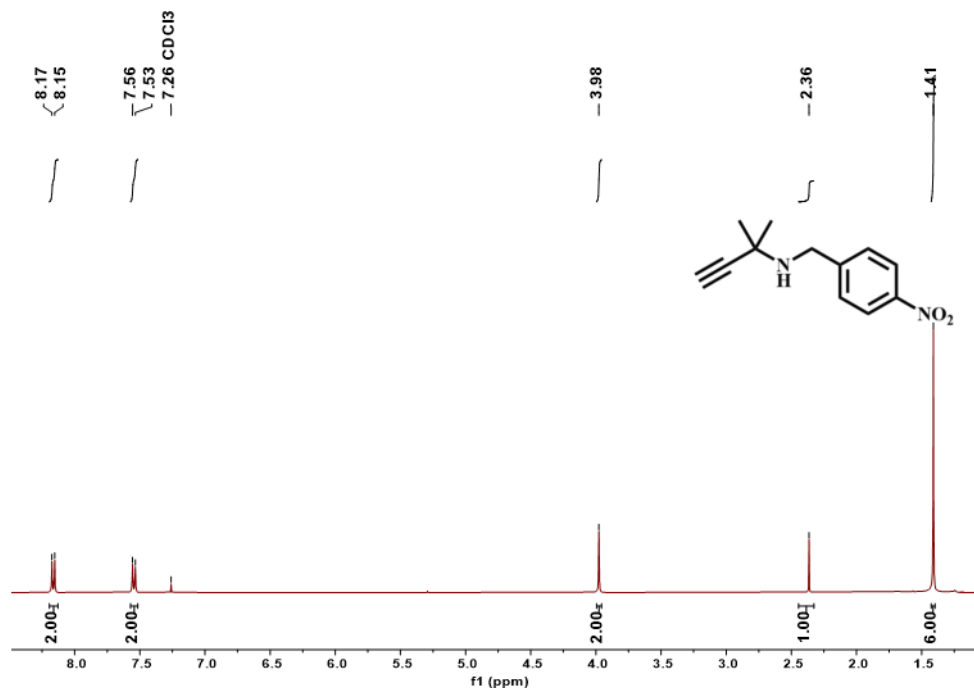
N-benzyl-2-methylbut-3-yn-2-amine (9a): ^1H NMR (400 MHz, Chloroform- d) δ 7.40 – 7.26 (m, 5H), 3.88 (s, 2H), 2.36 (s, 1H), 1.43 (s, 6H).



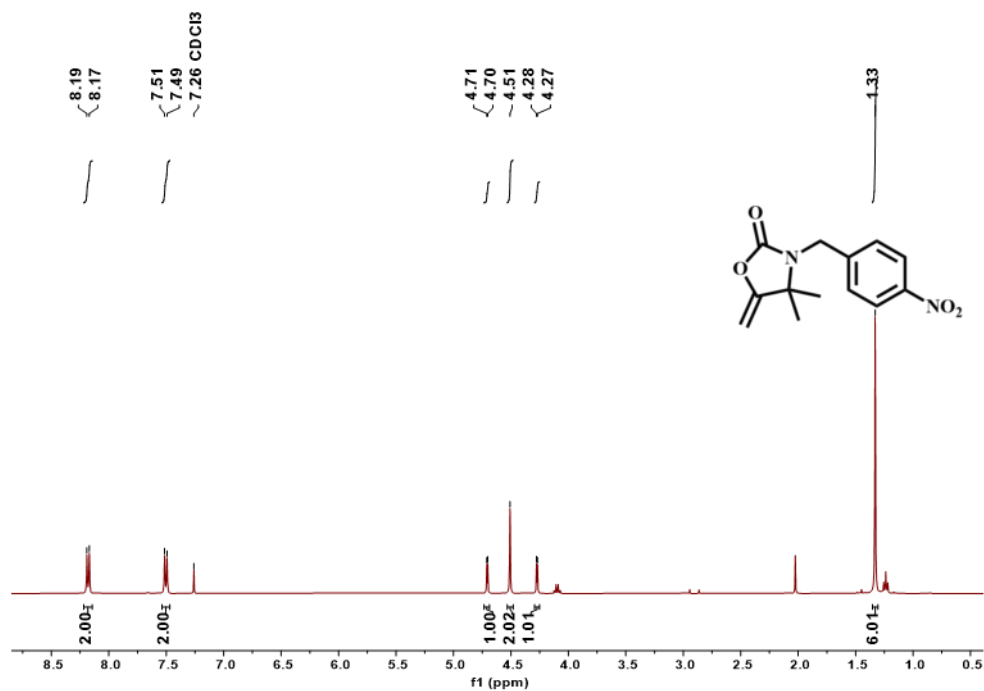
3-benzyl-4,4-dimethyl-5-methyleneoxazolidin-2-one (9b): ^1H NMR (400 MHz, Chloroform- d) δ 7.31 (dd, $J = 13.3, 5.8$ Hz, 5H), 4.66 (d, $J = 3.3$ Hz, 1H), 4.45 (s, 2H), 4.22 (d, $J = 3.3$ Hz, 1H), 1.30 (s, 6H).



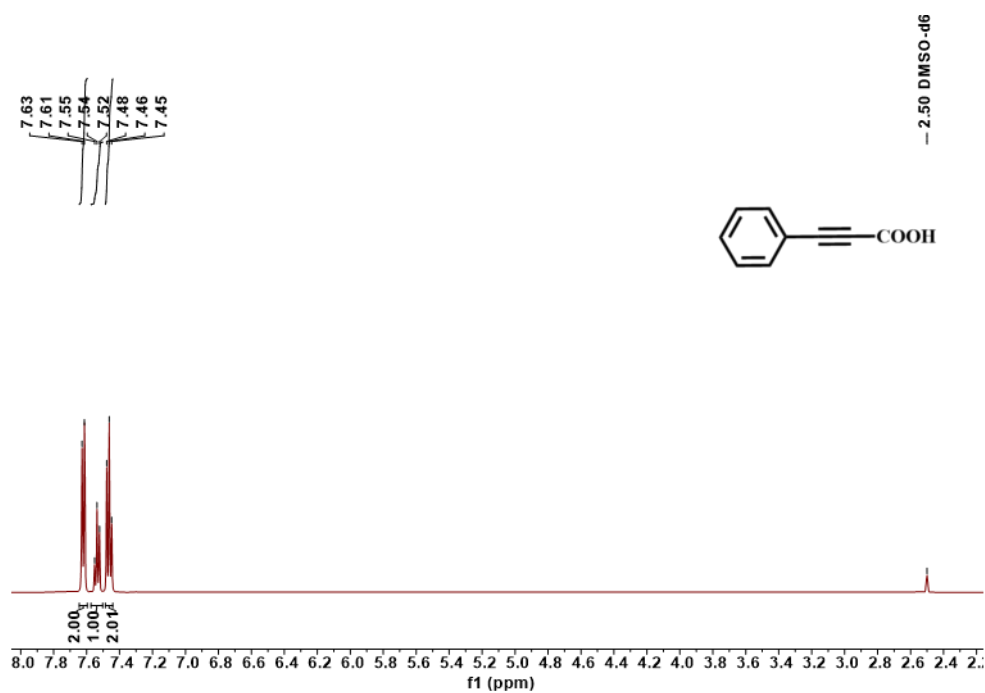
2-methyl-N-(4-nitrobenzyl) but-3-yn-2-amine (10a): ^1H NMR (400 MHz, Chloroform-*d*) δ 8.16 (d, $J = 8.7$ Hz, 2H), 7.55 (d, $J = 8.8$ Hz, 2H), 3.98 (s, 2H), 2.36 (s, 1H), 1.41 (s, 6H).



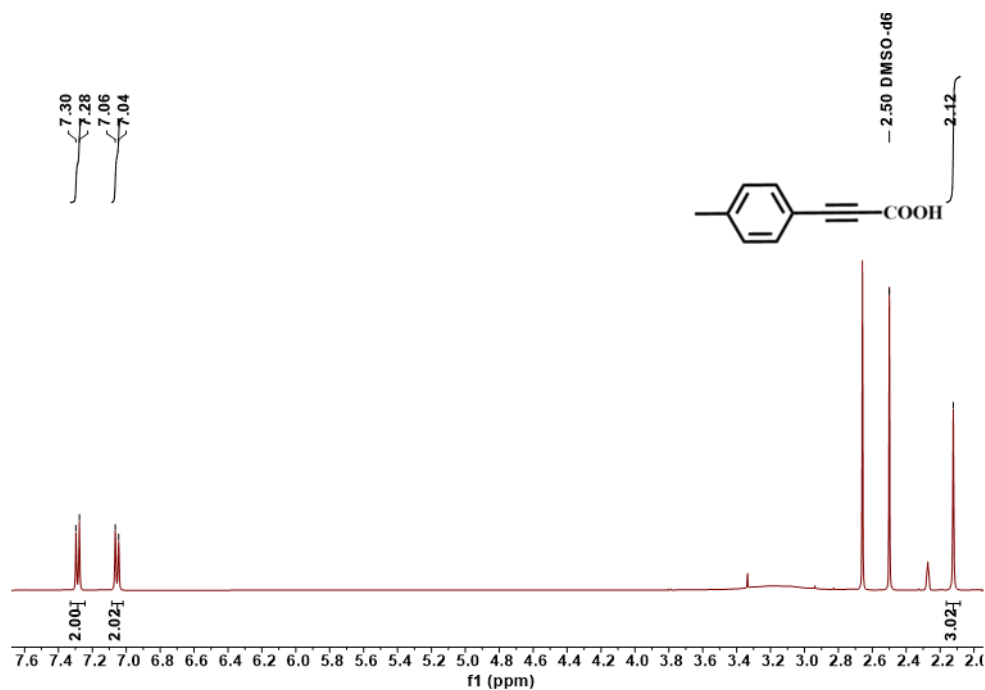
4,4-dimethyl-5-methylene-3-(4-nitrobenzyl) oxazolidin-2-one (10b): ^1H NMR (400 MHz, Chloroform-*d*) δ 8.18 (d, $J = 8.6$ Hz, 2H), 7.50 (d, $J = 8.5$ Hz, 2H), 4.71 (d, $J = 3.5$ Hz, 1H), 4.51 (s, 2H), 4.27 (d, $J = 3.5$ Hz, 1H), 1.33 (s, 6H).



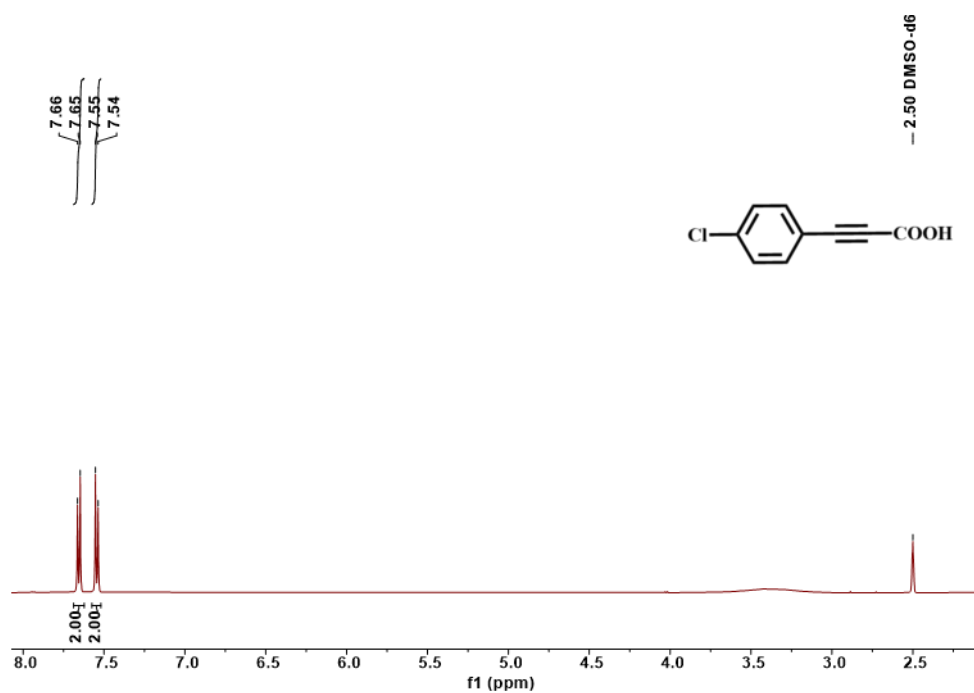
3-phenylpropionic acid(1d): ^1H NMR (400 MHz, $\text{DMSO-}d_6$) δ 7.62 (d, $J = 7.3$ Hz, 2H), 7.54 (t, $J = 7.5$ Hz, 1H), 7.46 (t, $J = 7.6$ Hz, 2H).



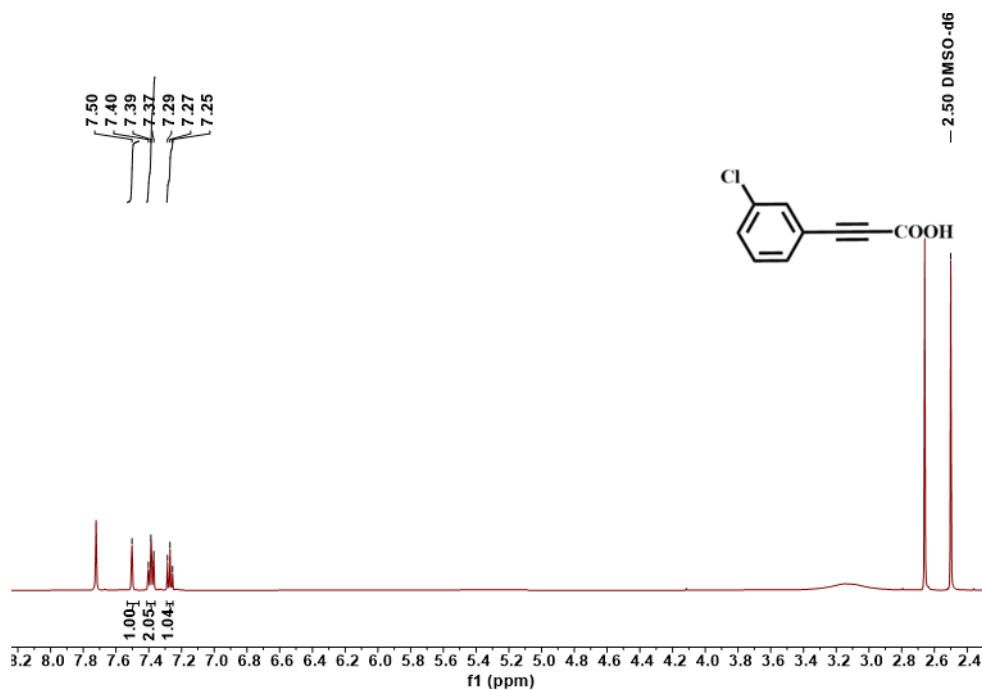
3-p-tolylpropionic acid(2d): ^1H NMR (400 MHz, $\text{DMSO-}d_6$): δ 7.29 (d, $J = 8.2$ Hz, 2H), 7.05 (d, $J = 7.9$ Hz, 2H), 2.12 (s, 3H).



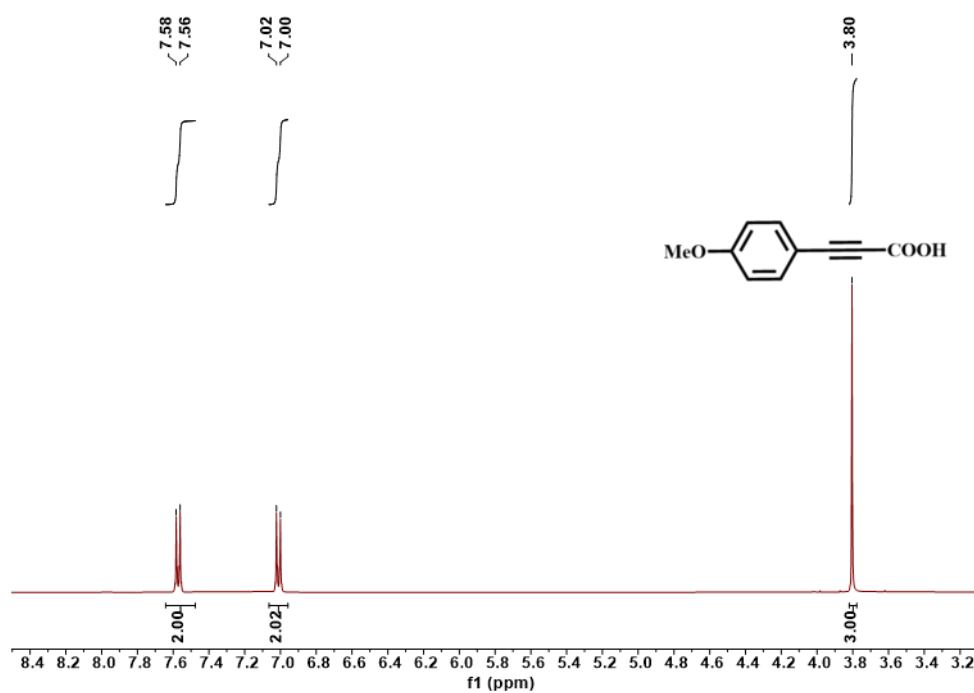
3-(4-chlorophenyl)propionic acid(3d): ^1H NMR (400 MHz, $\text{DMSO-}d_6$) δ 7.66 (d, $J = 8.5$ Hz, 2H), 7.54 (d, $J = 8.6$ Hz, 2H).



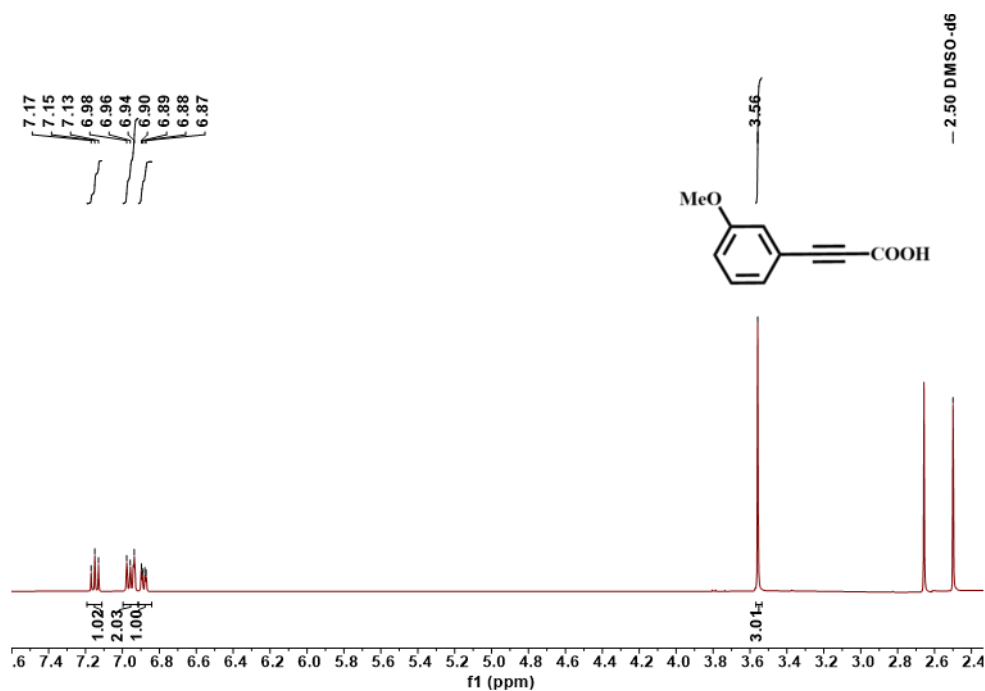
3-(3-chlorophenyl) propionic acid(4d): ^1H NMR (400 MHz, $\text{DMSO-}d_6$) δ 7.50 (s, 1H), 7.39 (t, $J = 8.5$ Hz, 2H), 7.27 (t, $J = 7.9$ Hz, 1H).



3-(4-methoxyphenyl) propiolic acid(5d): ^1H NMR (400 MHz, $\text{DMSO-}d_6$) δ 7.57 (d, $J = 8.8$ Hz, 2H), 7.01 (d, $J = 8.9$ Hz, 2H), 3.80 (s, 3H).



3-(3-methoxyphenyl) propiolic acid(6d): ^1H NMR (400 MHz, $\text{DMSO-}d_6$) δ 7.15 (t, $J = 7.9$ Hz, 1H), 7.00 – 6.92 (m, 2H), 6.88 (dd, $J = 7.4, 2.6$ Hz, 1H), 3.56 (s, 3H).



4. References

- [1] Y. Fu, D. Sun, Y. Chen, R. Huang, Z. Ding, X. Fu and Z. Li, *Angew. Chem., Int. Ed.*, 2012, **51**, 3364-3367.
- [2] X.-M. Cheng, P. Wang, S.-Q. Wang, J. Zhao and W.-Y. Sun, *ACS Appl. Mater. Interfaces*, 2022, 14, 32350-32359.
- [3] L. Wang, C. Qi, W. Xiong and H. Jiang, *Chin. J. Catal.*, 2022, **43**, 1598-1617.
- [4] J. Wu, S. Ma, J. Cui, Z. Yang and J. Zhang, *Nanomaterials*, 2022, **12(18)**, 3088
- [5] S. Ghosh, R. A. Molla, U. Kayal, A. Bhaumik and S. M. Islam, *Dalton Trans*, 2019, **48**, 4657-4666.
- [6] M. Zhao, S. Huang, Q. Fu, W. Li, R. Guo, Q. Yao, F. Wang, P. Cui, C. H. Tung and D. Sun, *Angew. Chem., Int. Ed.*, 2020, **59**, 20031-20036.
- [7] X. H. Liu, J. G. Ma, Z. Niu, G. M. Yang and P. Cheng, *Angew. Chem., Int. Ed.*, 2014, **54**, 988-991.
- [8] X. Xu, Z. Li, H. Huang, X. Jing and C. Duan, *Inorg. Chem. Front.*, 2022, **9**, 3839-3844.
- [9] A. L. Gu, Y. X. Zhang, Z. L. Wu, H. Y. Cui, T. D. Hu and B. Zhao, *Angew. Chem., Int. Ed.*, 2022, **61**, e202114817.
- [10] C.-H. Zhang, T.-D. Hu, Y.-T. Zhai, Y.-X. Zhang and Z.-L. Wu, *Green Chem.*, 2023, **25**, 1938-1947.
- [11] X. Wang, Z. Chang, X. Jing, C. He and C. Duan, *ACS Omega*, 2019, **4**, 10828-10833.
- [12] Z. Chang, X. Jing, C. He, X. Liu and C. Duan, *ACS Catal.*, 2018, **8**, 1384-1391.
- [13] M. Zhao, S. Huang, Q. Fu, W. Li, R. Guo, Q. Yao, F. Wang, P. Cui, C. H. Tung and D. Sun, *Angew. Chem., Int. Ed.*, 2020, **59**, 20031-20036.
- [14] Y. Yang, Y. Li, Y. Lu, Z. Chen and R. Luo, *ACS Catalysis*, 2024, **14**, 10344-10354.
- [15] J. Wu, S. Ma, J. Cui, Z. Yang and J. Zhang, *Nanomaterials*, 2022, **12(18)**, 3088.
- [16] Z. Qin, L. Wang, L. Chen, Y. Li and K. Shen, *Small*, 2024, **20**, 2403517.
- [17] N.-N. Zhu, X.-H. Liu, T. Li, J.-G. Ma, P. Cheng and G.-M. Yang, *Inorg. Chem.* 2017, **56**, 3414-3420.
- [18] J. Shi, L. Zhang, N. Sun, D. Hu, Q. Shen, F. Mao, Q. Gao and W. Wei, *ACS Appl. Mater. Interfaces.*, 2019, 11, 28858-28867.
- [19] X. H. Liu, J. G. Ma, Z. Niu, G. M. Yang and P. Cheng, *Angew. Chem., Int. Ed.*, 2014, **54**, 988-991.
- [20] G. Xiong, B. Yu, J. Dong, Y. Shi, B. Zhao and L.-N. He, *Chem. Commun.*, 2017, **53**, 6013-6016.
- [21] G. Singh, N. Duhan, T. J. Dhillip Kumar and C. M. Nagaraja, *ACS Appl. Mater. Interfaces.*, 2024, **16**, 5857-5868.
- [22] M. Trivedi, B. Bhaskaran, A. Kumar, G. Singh, A. Kumar and N. P. Rath, *New J. Chem.* 2016, **40**, 3109-3118.
- [23] Y. Yun, H. Sheng, K. Bao, L. Xu, Y. Zhang, D. Astruc and M. Zhu, *J. Am. Chem. Soc.*, 2020, **142**, 4126-4130.
- [24] R.-J. Wei, M. Xie, R.-Q. Xia, J. Chen, H.-J. Hu, G.-H. Ning and D. Li, *J. Am. Chem. Soc.*, 2023, **145**, 22720-22727.

- [25] C.-H. Zhang, T.-D. Hu, Y.-T. Zhai, Y.-X. Zhang and Z.-L. Wu, *Green Chem.*, 2023, **25**, 1938-1947.
- [26] P. García-Domínguez, L. Fehr, G. Rusconi and C. Nevado, *Chemical Science*, 2016, **7**, 3914-3918.
- [27] H. Mizoguchi, R. Watanabe, S. Minami, H. Oikawa and H. Oguri, *Org. Biomol. Chem.*, 2015, **13**, 5955-5963.